

pvCNN: Privacy-Preserving and Verifiable Convolutional Neural Network Testing

Jiasi Weng, Jian Weng*, *Member, IEEE*, Gui Tang, Anjia Yang, Ming Li, Jia-Nan Liu

Abstract—This paper proposes a new approach for privacy-preserving and verifiable convolutional neural network (CNN) testing, enabling a CNN model *developer* to convince a *user* of the truthful CNN performance over non-public data from *multiple testers*, while respecting model privacy. To balance the security and efficiency issues, three new efforts are done by appropriately integrating homomorphic encryption (HE) and zero-knowledge succinct non-interactive argument of knowledge (zk-SNARK) primitives with the CNN testing.

First, a CNN model to be tested is strategically partitioned into a private part kept locally by the model developer, and a public part outsourced to an outside server. Then, the private part runs over HE-protected test data sent by a tester, and transmits its outputs to the public part for accomplishing subsequent computations of the CNN testing. Second, the correctness of the above CNN testing is enforced by generating zk-SNARK based proofs, with an emphasis on optimizing proving overhead for two-dimensional (2-D) convolution operations, since the operations dominate the performance bottleneck during generating proofs. We specifically present a new quadratic matrix programs (QMPs)-based arithmetic circuit with a *single multiplication gate* for expressing 2-D convolution operations between multiple filters and inputs in a batch manner. Third, we aggregate multiple proofs with respect to a same CNN model but different testers' test data (*i.e.*, different statements) into one proof, and ensure that the validity of the aggregated proof implies the validity of the original multiple proofs. Lastly, our experimental results demonstrate that our QMPs-based zk-SNARK performs nearly $13.9\times$ faster than the existing QAPs-based zk-SNARK in proving time, and $17.6\times$ faster in Setup time, for high-dimension matrix multiplication.

I. INTRODUCTION

Convolutional neural networks (CNNs) [1], [2] have been widely applied in various application scenarios, such as healthcare analysis, autonomous vehicle and face recognition. But real-life reports demonstrate that neural networks often exhibit erroneous decisions, leading to disastrous consequences, *e.g.*, (r1) self-driving crash due to the failure of identifying unexpected driving environments [3], and (r2) social fighting derived from racial biases embedded in face recognition systems [4]. The reports emphasize that when applying CNN models in security-critical scenarios, especially for those from third-party developers, model users should be sufficiently cautious of benchmarking the CNN models to obtain the truthful multi-faceted performance, like robustness (in r1) and fairness (in r2), not limited to natural accuracy.

A widely adopted approach to benchmarking a CNN model is black-box testing [5], [6]. Black-box testing enables users to have a black-box access to the CNN model, that is, feeding the model with a batch of test data and merely observing its outputs, *e.g.*, the proportion of correct predictions. Such approach is suitable for the setting where model users and developers are not the same entities. The main reasons are that the parameters of CNN models are intellectual properties and are vulnerable to privacy attacks, such that developers are unwilling to reveal the parameters. We are also aware that existing excellent white-box testing approaches [7] can test CNN models in a fine-granularity fashion using model parameters, but black-box testing is preferred in the above setting where model parameters are inaccessible.

Starting by black-box testing, two essential issues need consideration to probe a CNN model's truthful multi-faceted performance. First, black-box testing strongly relies on the test datasets [7], and hence available test datasets should be as various as possible, so as to support testing a model's multi-faceted performance. One evidence is that multiple benchmarks are built by embedding dozens of types of noises into ImageNet to measure the robustness of CNN models [8]. Despite the necessity, building such benchmarks consumes many manpower and multi-party efforts, even for large companies, *e.g.*, a recent project named Crowdsourcing Adverse Test Sets for Machine Learning (CATS4ML) launched by Google AI. Thus, the off-the-shelf test datasets for supporting multi-faceted CNN testing are likely from multiple sources. Second, black-box testing also opens a door for untrusted third-party developers to cheat in testing. They might forge untruthful outputs without correctly running the processes of CNN testing on given test datasets. Additionally, if developers can in advance learn a given test dataset, they might craft a CNN which typically adapts to the test dataset, which deviates from our initial goal of testing their truthful multi-faceted performance. From this point, test datasets cannot be public, not merely due to that datasets themselves are privacy-sensitive in many security-critical scenarios. *Therefore, there needs an approach for users to validate the correctness of the black-box CNN testing over test datasets, in which test datasets are not public and the CNN is privacy-preserving.*

While many attractive efforts have been done to make CNN prediction/testing verifiable [9]–[16] using cryptographic proof techniques [17]–[22], we still need a new design satisfying our scenario requirements. We now clarify our scenario requirements, and explain why previous works are not really satisfactory to the requirements. As demonstrated in Fig. 1, a publicly accessible platform (in gray color), *e.g.*, ModelZoo

J.s. Weng, J. Weng, G. Tang, A. Yang, M. Li and J.n. Liu are with the College of Cyber Security, Jinan University, Guangzhou 510632, China. E-mail: wengjiasi@gmail.com, cryptjweng@gmail.com, guitang001@gmail.com, anjiayang@gmail.com, limjnu@gmail.com, j.n.liu@foxmail.com. Jian Weng is the corresponding author.

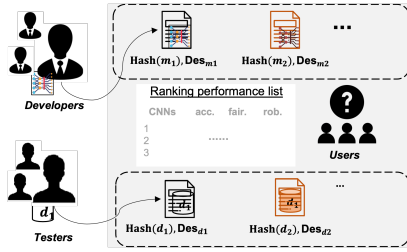


Fig. 1. Scenario example (m_1, m_2 refer to CNN models, and d_1, d_2 refer to test datasets; Des means non-private descriptions for the CNN models or test datasets).

[23] and Kaggle [24], can allow third-party *developers* to advertise their CNN models towards users for earning profits. For *users* who will pay for a CNN model, they have a natural concern on the CNN model's truthful performance, taking into account the aforementioned reports. To address the concern, the platform can announce a crowdsourcing task to test the CNN model, such that *testers* participate in probing the model performance using their test datasets. Note that both the model parameters and test datasets are not revealed on the platform while the model structures (see Section II-A) can be public. Considering the presence of an untrusted CNN developer, our design empowers him/her with a proving ability to convince a later-coming user of the truthful CNN performance over given multi-tester test datasets, satisfying three requirements as follows:

(a) **Public verifiability and no need of interaction.** Since the user is later-coming and not pre-designated, proof generation and verification w.r.t the CNN testing should not share private information between the developer (*i.e.*, prover) and the user (*i.e.*, verifier), and thereby requiring public verifiability. The proving ability should also be non-interactive, due to that the CNN developer, the user and testers are not always simultaneously online.

(b) **Privacy preservation.** During the CNN testing, model parameters should not be exposed except the CNN developer himself, since the parameters memorize sensitive training data [25], and they are intellectual properties. Also, the test data should also be protected against the CNN developer, considering the CNN developer might strategically craft the CNN model based on the test data. Besides, any verifier should fail to learn private information from the final CNN performance and proofs.

(c) **Batch proving and verification.** A testing CNN model usually receives test data in batches, so it is a natural requirement to support batch operations in proof generation. In terms of verification in our scenario, a later-coming user has to verify multiple proofs w.r.t a single CNN model which is tested with the multi-tester test data. Hence, enabling the user to verify multiple proofs in a batch manner can be another desirable requirement.

Previous Works. Recently many verifiable CNN prediction/testing schemes [9]–[16] have proposed creative designs from various technical perspectives to enforce the correctness of CNN prediction/testing, but they cannot fully satisfy our requirements, as summarized in TABLE I. The previous schemes can be roughly classified into two major groups, according to their underlying cryptographic proof techniques, such as Sum-Check like protocols [17], [26], [27] and zk-SNARK like sys-

TABLE I
COMPARISON OF VERIFIABLE CNN PREDICTION/TESTING SCHEMES. CONSIDER A TWO-DIMENSIONAL (2-D) CONVOLUTION APPLYING TO A FILTER MATRIX OF $m \times m$ AND A TEST DATA MATRIX OF $n \times n$. THE COLUMN OF PROVING TIME IS FOR SUCH 2-D CONVOLUTIONS ON M FILTER MATRICES AND Mn^2 TEST DATA MATRICES (UNDER PLAINTEXT). FOR SIMPLICITY, WE NOTE $M > m$ AND THE CHANNEL NUMBER OF TEST DATA IS 1.

Schemes	Requirement			Proving Time
	(a)	(b)	(c)	
Safetynets [9]	○	○	○	$O(M \cdot Mn^2 \cdot (n^2 \cdot m^2))$
Keuffer's [13]	●	●	○	$O(M \cdot Mn^2 \cdot (n^2 \cdot m^2))$ [11]
SafeTPU [10]	○	○	●	$O(M \cdot Mn^2 \cdot (n^2 \cdot m^2 \cdot \frac{m^2}{n^2}))$
Madi's [15]	○	●	○	$O(M \cdot Mn^2 \cdot (n^2 \cdot m^2))$
vCNN [11]	●	●	○	$O(M \cdot Mn^2 \cdot (n^2 + m^2))$
VeriML [14]	●	●	○	$O(M \cdot Mn^2 \cdot (n^2 \cdot m^2))$ [11]
ZEN [12]	●	●	●	$O(M \cdot Mn^2 \cdot (n^2 \cdot m^2 \cdot \frac{1}{n^2}))$
zkCNN [16]	○	●	○	$O(M \cdot Mn^2 \cdot (n^2 + m^2))$
Ours	●	●	●	$O(Mn^2)$

○ denotes the requirement is not satisfied;

● denotes the scheme partially supports the requirement;

● denotes the scheme fully supports the requirement.

tems (zk-SNARK, zero-knowledge Succinct Non-interactive ARGument of Knowledge) [18]–[22]. Based on the underlying techniques, some schemes clearly elaborate how they support privately verifiable and interactive proofs [9], [10], [15]; some schemes support partial privacy protection [11], [12], [15]; also, most schemes do not require a batch manner [9], [11], [13]–[16]. In addition, a few of works [28], [29] do not focus on CNNs. Among these, zkCNN [16] is the latest scheme based on Sum-Check like protocols, while the state-of-the-art schemes built on zk-SNARKs are vCNN [11] and ZEN [12]. Taking into account our **requirement (a)**, our work follows vCNN and ZEN to adopt zk-SNARK systems, precisely speaking, Groth16 zk-SNARK [18]. It is the most efficient general-purpose zk-SNARK system, supporting many properties we desire, including public delegatability, public verifiability, succinctness and zero-knowledgeness. Recently, Fiore et al. [21] leverage an efficient commit-and-prove variant of Groth16 zk-SNARK to instantiate a new zk-SNARK system for efficiently verifiable computation over polynomial rings, *e.g.*, encrypted data by a leveled fully homomorphic encryption (FHE) algorithm. Despite the merits, zk-SNARK systems incur unaffordable costs for a prover in proof generation, as mentioned by vCNN [11], ZEN [12] and zkCNN [16]. Hence, our work also proposes a new method to reduce the proof generation overhead for verifiable CNN testing based on zk-SNARKs.

While many existing schemes improve proving time for convolutional operations which dominate the major computation of a CNN prediction/testing, there still leaves improvement space when considering **requirement (c)**. As compared in TABLE I, despite that vCNN [11] and zkCNN [16] reduce the proving time of a 2-D convolution between a $m \times m$ filter matrix and a $n \times n$ test input matrix to $O(n^2 + m^2)$, they still need $O(M \cdot Mn^2 \cdot (n^2 + m^2))$ proving time for handling 2-D convolution operations over M filters and Mn^2 test inputs. Our work focuses on such case, and reduces the proving time to $O(Mn^2)$. We remark that ZEN's [12] zk-SNARK friendly optimization techniques can be complementary to our work, since we use the similar unsigned quantization method and Groth16 zk-SNARK as it. Another promising work can be followed is Mystique [30], which leverages subfield vector oblivious linear evaluation based interactive ZK protocols to

support verifiability of complicated neural network prediction.

Our Designs. To satisfy our three requirements, our designs include three components: (1) privacy-preserving CNN testing based on FHE and a *model splitting* strategy, (2) generating zk-SNARK proofs for the above privacy-preserving CNN testing, with an emphasis on proposing a new quadratic matrix programs (QMPs) zk-SNARK for proving 2-D convolutional operation relations, and (3) enabling zk-SNARK proof aggregation for verifying multiple proofs in a batch manner.

Firstly, we start by letting a developer locally run the CNN testing process over FHE-protected test data from every tester. While FHE can provide stronger data confidentiality, compared to other secure computing techniques, such as secure multi-party computation and differential privacy [31], the straightforward adoption is computation-expensive, nearly 4 to 5 orders slower than computing on plaintext data. Moreover, proving overhead on encrypted data (in ring field \mathcal{R}_q) and encoded CNN parameters (in ring field \mathcal{R}_t) is unaffordable and impractical. We hence find a middle point to realize the FHE-based CNN testing, by introducing a strategy of model splitting [32], so as to balance privacy and efficiency. Particularly, the CNN developer can split his CNN model into two parts: one is private, called PriorNet, and another one is public, called LaterNet. Then, the developer can locally evaluate PriorNet on the FHE-protected test data, and outsource LaterNet to the computation-powerful cloud for accomplishing the subsequent computation by feeding it with the plaintext outputs of PriorNet. Next, due to that the plaintext outputs of PriorNet might be susceptible to model inversion attacks [32], we can further carefully select an optimized split point [32], so as to prevent the PriorNet's outputs from disclosing private information.

The second step is to prove the correctness of the above splitting CNN testing on FHE-encrypted test data. We concretely adopt a proving roadmap recently proposed by Fiore *et al.* [21], in which Step 1 is to prove the simultaneous evaluation of multiple polynomial ring elements in the same randomly selected point (for PriorNet), and Step 2 is to prove the satisfiability of QAPs-based arithmetic circuits (for PriorNet and LaterNet) whose inputs and outputs are committed.

But we do not directly apply Step 2 into our case, since the direct adoption causes high proving and storage overhead due to a large number of multiplication gates when handling convolution operation relations [11]. We thus present a new method to reduce the number of multiplication gates during proof generation, for improving the proving time of the convolutional operation relations. At first, we represent the 2-D convolution operations between M filters which are $m \times m$ matrices and Mn^2 test inputs which are $n \times n$ matrices into **a single matrix multiplication (MM)** computation. The MM computation is conducted between a $Mn^2 \times Mn^2$ filter matrix which is strategically assigned with the M filters and zeros as padding for operation correctness, and another $Mn^2 \times Mn^2$ input matrix which is assigned with the Mn^2 test inputs. After that, we start from QAPs-based zk-SNARKs and present a new QMP formula [33]. We then express the above single MM computation as a circuit over $Mn^2 \times Mn^2$ matrices **by only one-degree QMPs**. As a result, the number of multiplication

gates always is 1 and the proving time linearly increases by the matrix dimension, *i.e.*, Mn^2 . With the efforts, we prove the satisfiability of the QMPs-based circuits via checking the divisibility in randomly selected point of the set of matrix polynomials of the QMPs. Note that there are heterogeneous operations in each neural network layer during CNN testing. We express the convolution and full connection operations as QMPs-based circuits, and ReLU and max pooling operations as QAPs-based circuits, and then separately generate specialized proofs for them. Furthermore, we add commit-and-prove components based on LegoSNARK [20] for gluing the separately generated specialized proofs, aiming to prove that the current layer indeed takes as inputs the previous layer's outputs.

Thirdly, we enable batch verification via proof aggregation, and only a single proof is generated for a tested CNN model. We aggregate multiple proofs with regard to the same CNN but different test inputs from multiple testers based on Snarkpack [34]. We note that the aggregation computation and proof validation can be delegated to computation-powerful parties in a competition manner, *e.g.*, decentralized nodes who run a secure consensus protocol. The validation result will be elected according to the consensus protocol, and then uploaded to the public platform and attached to the corresponding CNN model. To the end, a future user who is interested in the CNN model can enjoy a lightweight verification by merely checking the validation result, via browsing the platform.

As for experiments, we present a proof-of-concept implementation, and evaluate the implementation. Our QMPs-based method for matrix multiplication performs about $17.6 \times$ faster than the existing QAPs-based method in Setup time, and $13.9 \times$ faster in proving time. We can also handle the matrix multiplication in dimensions more than 220×220 while the matrix dimension the previous QMPs-based method can handle is limited to 220×220 [13]. However, our proof size is 2 or 3 orders larger than that of the QAPs-based zk-SNARK. Despite the demerit, we observe that the order of magnitude becomes smaller with an increasing number of multiplications, which demonstrates our method can be more suitable to handle the computation involving in a large number of multiplications.

II. PRELIMINARIES

A. CNN Prediction

We present here a prediction process of LeNet-5 which is a simple CNN on a step-by-step basis. LeNet-5 basically contains two convolution (conv) layers and three full connection (fc) layers in order; other layers between them include activation (act) and max pooling or average pooling (pool) layers, and the output layer is softmax layer. Note that more complex CNNs generally contain the above layers. Taking as inputs a single-channel test data \mathbf{X} which is a $n \times n$ matrix, *e.g.*, gray-scale image, the layer-by-layer operations are conducted sequentially: $y_o = f^o(f^{fc}(f^{fc}(f^{pool}(f^{act}(f^{conv}(f^{pool}(f^{act}(f^{conv}(\mathbf{X}))))))))))$, where f^o is the output function which selects out the maximal value among the values outputted by the last f^{fc} , determining the prediction output.

We proceed to elaborate the layer-by-layer operations in detail. Denote a $m \times m$ weight matrix $\mathbf{W}^{(k)}$ in the k_{th} layer.

(a) **Layer f^{conv} :** Two dimension (2-D) convolution operations will be applied to input matrices and weight matrices (also called *filters*). Here, we show a 2-D convolution operation applying to two matrices \mathbf{X} and $\mathbf{W}^{(1)}$ with a $(n - m + 1) \times (n - m + 1)$ matrix $\mathbf{Y}^{(1)}$ as output:

$$\mathbf{Y}^{(1)}[i][j] = \sum_{l_r^{(1)}=0, l_c^{(1)}=0}^{m-1, m-1} \mathbf{X}[i + l_r^{(1)}][j + l_c^{(1)}] \times \mathbf{W}^{(1)}[l_r^{(1)}][l_c^{(1)}],$$

where $i, j \in [0, n - m + 1)$ and the row (resp. column) index of the weight is $l_r^{(1)}$ (resp. $l_c^{(1)}$), and the stride size is 1. The subsequent f^{conv} are done similarly, applying to the previous layer's output matrices and the weight matrices in the current layer.

(b) **Layer f^{act} :** There are two widely used activation functions, applying to each element of the output matrices of f^{conv} in layer l , in order to catch non-linear relationships. Concretely, the two functions are $f^{act}(\mathbf{Y}^{(k)}[i][j]) = \max(\mathbf{Y}^{(k)}[i][j], 0)$ named ReLU function, and $f^{act}(\mathbf{Y}^{(k)}[i][j]) = \frac{1}{1 + e^{-\mathbf{Y}^{(k)}[i][j]}}$ named Sigmoid function.

(c) **Layer f^{pool} :** Average pooling and max pooling are two common pooling functions for reducing the dimension of the output matrices in certain layer k . They are applied to each region covered by a $m \times m$ filter, within each output matrix of the previous f^{act} layer. Specifically, average pooling function is done by $(\mathbf{Y}^{(k)}[0][0], \dots, \mathbf{Y}^{(k)}[m-1][m-1])/m^2$, and max pooling function is by $\max(\mathbf{Y}^{(k)}[0][0], \dots, \mathbf{Y}^{(k)}[m-1][m-1])$.

(d) **Layer f^{fc} :** In this layer, each output matrix of the previous layer multiplies by each weight matrix, and then add with a bias in the current layer. We will omit the bias, for simplicity.

After executing the mentioned sequential operations, f^o finally outputs a label l_{test} for \mathbf{X} , which is the prediction output.

B. Non-Interactive Zero-Knowledge Arguments

Non-interactive zero-knowledge (NIZK) arguments allow a prover to convince any verifier of the validity of a statement without revealing other information. Groth [18] proposed the most efficient zk-SNARK scheme, with small constant size and low verification time. Our work leverages a *commit-and-prove* (CaP) Groth16 variant to prove arithmetic circuit satisfiability in our verifiable CNN testing scenario, where inputs, parameters and outputs are committed. We highlight the usability of the CaP functionality for our scenario in Appendix A. We here recall some essential preliminaries.

Bilinear groups. Here introduces Type-3 bilinear group (p, G_1, G_2, G_T, e) , where p is a prime, and G_1, G_2 are cyclic groups of prime order p . Note that $g \in G_1, h \in G_2$ are the generators. Then, $e : G_1 \times G_2 \rightarrow G_T$ is a bilinear map, that is, $e(g^a, h^b) = e(g, h)^{ab}$, where $a, b \in \mathbb{Z}_p, e(g, h)^{ab} \in G_T$.

Arithmetic circuits. Arithmetic circuits are the widely adopted computational models for expressing the computation of polynomials over finite fields. An arithmetic circuit is formed with a directed acyclic graph, where each vertex of fan-in two called *gate* is labeled by an operation, and each edge called *wire* is labeled by an operand in the finite field. We review the arithmetic circuit definition as follows:

Definition. Given an arithmetic circuit $\phi_{AC} : \mathbb{F}_p^{n_{in}} \rightarrow \mathbb{F}_p^{n_{ot}}$, taking as inputs n_{in} variables or constants from the finite field \mathbb{F}_p , and executing the operations sum or product via its vertices, which returns n_{ot} values in \mathbb{F}_p as outputs. Herein, p is an appropriate modulus.

Based on the above definition, we note that the arithmetic circuit's input wires and output wires are labeled by given n_{in} inputs and n_{ot} outputs correspondingly; its gates can be labeled by a set of operations $\{+, \times\}$, usually named as addition gates and multiplication gates. Besides, note that there are usually two measures for the complexity of a circuit, such as its size and depth. Specifically, the number of wires of the circuit determines its size; the longest path from inputs to the outputs determine its depth.

Arbitrary arithmetic circuits can be naturally formulated as a set of quadratic arithmetic programs [35]. We introduce the definition of QAPs here. The complementary description about arithmetic constraint systems for QAPs refer to Appendix B. More details to build QAPs for arithmetic circuits can be founded in [35].

Quadratic arithmetic program (QAP). For an arithmetic circuit with n_{in} input variables, n_{ot} output variables in \mathbb{F}_p (p is a large prime) and n_* multiplication gates, a QAP is consisting of three sets of polynomials $\{l_i(X), r_i(X), o_i(X)\}_{i=0}^m$ and a n_* -degree target polynomial $t(X)$. The QAP holds and $(a_0, \dots, a_{n_{in}}, a_{m-n_{ot}+1}, \dots, a_m) \in \mathbb{F}_p^{n_{in}+n_{ot}}$ is valid assignment for the input/output variables of the arithmetic circuit *iff* there is $(a_{n_{in}+1}, \dots, a_{m-n_{ot}}) \in \mathbb{F}_p^{m-n_{in}-n_{ot}}$ such that $\sum_{i=0}^m a_i l_i(X) \cdot \sum_{i=0}^m a_i r_i(X) \equiv \sum_{i=0}^m a_i o_i(X) \pmod{t(X)}$. Herein, the size of the QAP is m and the degree is n_* .

zk-SNARKs. Groth16 scheme is a QAPs-based zk-SNARK, enabling proving the satisfiability of QAPs via conducting a divisibility check between polynomials, which is equivalent to prove the satisfiability of the corresponding circuits.

Now, we figure out some notations which can pave the way for presenting Groth16 and our design later. Concretely, we can specify the mentioned assignment $(a_0, \dots, a_{n_{in}}, a_{m-n_{ot}+1}, \dots, a_m) \in \mathbb{F}_p^{n_{in}+n_{ot}}$ as **statement** \mathbf{st} to be proven, and specify $(a_{n_{in}+1}, \dots, a_{m-n_{ot}}) \in \mathbb{F}_p^{m-n_{in}-n_{ot}}$ as **witness** \mathbf{wt} only known by a prover. Then, we define the polynomial time computable binary **relation** \mathbf{R} that comprises the pairs of $(\mathbf{st}, \mathbf{wt})$ satisfying the denoted QAP $\{\{l_i(X), r_i(X), o_i(X)\}_{i \in [0, m]}, t(X)\}$. If \mathbf{R} holds on $(\mathbf{st}, \mathbf{wt})$, $\mathbf{R} = 1$; otherwise, $\mathbf{R} = 0$. Formally, the relation is denoted as $\mathbf{R} = \{(\mathbf{st}, \mathbf{wt}) \mid \mathbf{st} := (a_0, \dots, a_{n_{in}}, a_{m-n_{ot}+1}, \dots, a_m), \mathbf{wt} := (a_{n_{in}+1}, \dots, a_{m-n_{ot}})\}$. Associated to the relation \mathbf{R} , we denote that **language** \mathbf{L} contains the statements that the corresponding witnesses exist in \mathbf{R} , that is, $\mathbf{L} = \{\mathbf{st} \mid \exists \mathbf{wt} \text{ s.t. } \mathbf{R}(\mathbf{st}, \mathbf{wt}) = 1\}$.

Based on the above notations, we are proceeding to review the definition of a zk-SNARK scheme for the relation \mathbf{R} . Specifically, a zk-SNARK scheme is consisting of a quadruple of probabilistic polynomial time (PPT) algorithms (Setup, Prove, Verify, Sim) as following:

- **Setup**($1^\lambda, \mathbf{R}$) \rightarrow (crs, td): the Setup algorithm takes a security parameter λ and a relation \mathbf{R} as inputs, which returns a common reference string crs and a simulation trapdoor td.

- $\text{Prove}(\text{crs}, \text{st}, \text{wt}) \rightarrow \pi$: the Prove algorithm takes crs , statement st and witness wt as inputs, and outputs an argument π .
- $\text{Verify}(\text{R}, \text{crs}, \text{st}, \pi) \rightarrow 0/1$: the Verify algorithm takes the relation R , common reference string crs , statement st and argument π as inputs, and returns 0 as **Reject** or 1 as **Accept**.
- $\text{Sim}(\text{R}, \text{td}, \text{st}) \rightarrow \pi'$: the Sim algorithm takes the relation R , simulation trapdoor td and statement st as inputs, and returns an argument π' .

Formally, a zero-knowledge proof system satisfies the following three properties.

- **Completeness.** Given a security parameter λ , $\forall (\text{st}, \text{wt}) \in \text{R}$, a honest prover can convince a honest verifier the validity of a correctly generated proof with an overwhelming probability, that is, $\Pr\{\text{Setup}(1^\lambda, \text{R}) \rightarrow (\text{crs}, \text{td}), \text{Prove}(\text{crs}, \text{st}, \text{wt}) \rightarrow \pi \mid \text{Verify}(\text{R}, \text{crs}, \text{st}, \pi) \rightarrow 1\} = 1 - \text{negl}(1^\lambda)$.
- **Computational soundness.** For every computationally bounded adversary \mathcal{A} , if an invalid proof is successfully verified by a honest verifier, there exists a PPT extractor \mathcal{E} who can extract wt with a non-negligible probability, that is, $\Pr\{\exists (\text{st}, \text{wt}) \notin \text{R}, \mathcal{A}(\text{crs}, \text{st}, \text{wt}) \rightarrow \pi \mid \text{Verify}(\text{R}, \text{crs}, \text{st}, \pi) \rightarrow 1 \wedge \mathcal{E}(\text{crs}) \rightarrow \text{wt}\} = 1 - \text{negl}(1^\lambda)$.
- **Zero-knowledge.** For every computationally bounded distinguisher \mathcal{D} , there exists the Sim algorithm such that \mathcal{D} successfully distinguishes a honestly generated proof from a simulation proof with a negligible probability, that is, $\Pr\{\text{Setup}(1^\lambda, \text{R}) \rightarrow (\text{crs}, \text{td}), \text{Prove}(\text{crs}, \text{st}, \text{wt}) \rightarrow \pi, \text{Sim}(\text{R}, \text{td}, \text{st}) \rightarrow \pi' \mid \mathcal{D}(\pi, \pi') = 1\} \leq \text{negl}(1^\lambda)$.

III. OVERVIEW

A. Basic Workflow

Fig. 2 demonstrates an overview of our pvCNN. There are five entities—public platform (PP), model tester (MT), model developer (MD), service provider (SP) and decentralized nodes (DN).

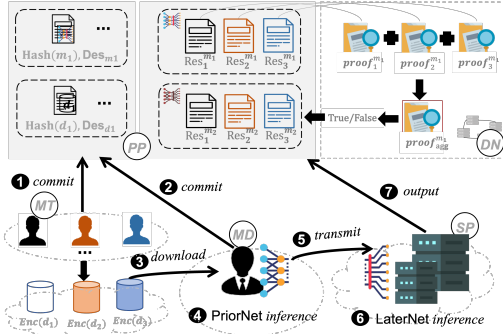


Fig. 2. Overview of pvCNN

PP is a publicly accessible platform like ModelZoo [23], Kaggle [24], and blockchain-enabled OpenMined or DecentralizedML. It can enable third-party **MD** (resp. **MT**) to advertise their pre-trained CNNs (resp. test data) on the platform, via announcing some usage descriptions and performance, so as to attract users (resp. **MD**) of interest, for earning profits. In order to convince future users, our pvCNN aims to empower **PP** with verifiable announcements, specifically focusing on verifiable CNN performance over test data. **MT** can freely participate in the **PP** by uploading some descriptions about their test data, when they are interested in certain pre-trained CNNs on

the **PP**. They can in advance store test data in an encryption manner on the publicly accessible cloud. **MD** can advertise their pre-trained CNNs on the **PP** without exposing the CNN parameters. In order to truthfully advertise their CNN models for future profits, they can download **MT**'s test data from the cloud to test their CNNs and announce verifiable performance results on the **PP**. **SP** can provide powerful computational and storage resources for **MD**. **DN** can be the computational nodes composing of a committee maintained by a secure consensus mechanism, e.g., permissioned blockchain nodes.

Next, the basic workflow around the above five entities contains seven steps: ❶ **MT** commits to test inputs on the **PP**; ❷ **MD** splits his CNN into **PriorNet** which is kept at local device and **LaterNet** which is sent to the **SP**, and meanwhile, submits two commitments to **PriorNet** plus **LaterNet** on the **PP**; ❸ **MT** sends test inputs encrypted by a leveled FHE (L-FHE) scheme [36] used to test the CNN to the **MD**, and proves that the encrypted test inputs are indeed the committed ones in Step ❶; ❹ **MD** evaluates the plaintext **PriorNet** on encrypted test inputs and generates a proof for convincing that he correctly performs **PriorNet** committed to in Step ❷ with the encrypted test inputs from the **MT**; ❺ **MD** sends the encrypted output of **PriorNet** inference to the **SP**, and commits to the output. Note that the encrypted output can be transformed into the ciphertext under the **SP**'s public key via re-encryption; ❻ **SP** successively runs **LaterNet** inference in the clear by taking the plaintext output of **PriorNet** inference as inputs, and proves that **LaterNet** is executed correctly with the true inputs and meanwhile **LaterNet** is consistent to the one committed before; ❼ **SP** submits the final test results (e.g., classification correctness rate) to the **PP**, and distributes proofs to a group of **DN** for proofs aggregation and validation.

B. Threat Assumptions

Developers. We consider CNN developers are untrusted; they can provide untruthful prediction results, e.g., outputting meaningless predictions or not using given test data for testing. They can also be curious about test data during a CNN testing. Note that our verifiable computing design does not focus on poisoned or backdoored models [37], but it greatly relies on multi-tester test data to probe the performance of CNN models in a black-box manner. Recently, SecureDL [38] and VeriDeep [39] resort to sensitive samples to detect model changes, which can be complementary to our work.

Service providers. They can be computationally powerful entities, and accept outsourced **LaterNet** from developers. Despite service providers' powerful capabilities on computation and storage, we do not trust them. They can try their best to steal private information with regard to CNNs and test inputs. They even incorrectly run **LaterNet** and produce untruthful or meaningless results for saving computation and storage resources. Service providers can also collude with a developer to fake correctness proofs, with respect to the independent inference processes based on a splitting CNN, aiming to evade verification by later-coming users.

Testers. Testers are organized via a crowdsourcing manner. We consider that the testers are willing to contribute their test

inputs for measuring the quality of the CNNs. A tester's test inputs concretely contain a batch of data on an input-label basis. We assume the original inputs need protected but their labels can be public (refer to encrypted inputs and plaintext labels in section IV-A). We also assume each label is consistent with the corresponding input's true label, considering currently popular crowdsourcing-empowered label platforms.

Decentralized computational nodes. We assume that the computational nodes follow a correct consensus protocol and no more than $1/3$ nodes are corrupted. Some permissioned blockchains, *e.g.*, Hyperledger Fabric and Corda.

IV. CONCRETE DESIGN

This section will introduce how to generate publicly verifiable proofs using zk-SNARKs for privacy-preserving CNN testing based on L-FHE and model splitting. To begin with, we introduce a splitting CNN testing. We enable a CNN developer to split his CNN into private and public parts. The private part is locally evaluated upon receiving the test data encrypted by testers. Then, the public part can be delegated to the service provider, so as to successively accomplish the subsequent operations, by taking the private part's output as input. With respect to the splitting CNN testing process, we next introduce how to generate correctness proofs against the untrusted developer and service provider. We particularly design three key components, including (i) *optimizing matrix multiplication relation*, (ii) *linking together correctness proofs for the splitting CNN testing*, and (iii) *aggregating proofs*.

A. Separate CNN Testing

Recent work [32] studies how to split a neural network into separate parts. We specifically take a simple CNN LeNet-5 for image classification as an example, and split it into two parts, following He *et. al* [32]'s method. Recall that we elaborate the prediction process of LeNet-5 in Section II-A. We choose the 2_{st} convolution layer as a split point, such that LeNet-5 can be partitioned into PriorNet $F_{M_1} = f^{pool}(f^{act}(f^{conv}(\cdot)))$ and LaterNet $F_{M_2} = f^o(f^{fc}(f^{fc}(f^{pool}(f^{act}(f^{conv}(\cdot)))))$. Suppose that the chosen split point is sufficiently optimized for privacy protection, and thus LaterNet can be public. We note that here M_1 and M_2 are the parameters of PriorNet and LaterNet, respectively.

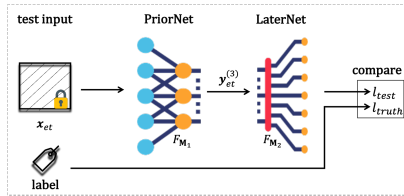


Fig. 3. Pipeline of PriorNet and LaterNet inference.

On top of such splitting, we elaborate in Fig. 3 the pipeline of PriorNet and LaterNet prediction over a given test input encrypted under the tester's public key via an L-FHE scheme, *e.g.*, BFV. We note that the corresponding label of the test input is not encrypted. Concretely, PriorNet is privately performed by the developer; it takes as input an encrypted test $x_{et} \in \mathcal{R}_q$, and produces an encrypted intermediate result $y_{et}^{(3)} \in \mathcal{R}_q$ as

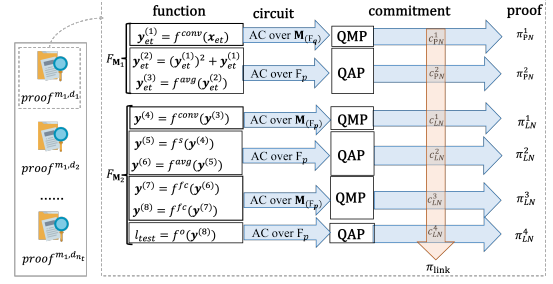


Fig. 4. Overview of proof generation.

the output. Since the activation layer within the PriorNet is non-linear, we replace it with a 2-degree polynomial function, which is a widely adopted method for adapting to the L-FHE scheme [31], [40].

Successively, $y_{et}^{(3)}$'s plaintext $Y^{(3)}$ will be fed into the LaterNet F_{M_2} whose computations are delegated to the service provider. We can leverage re-encryption technique to let the service provider obtain the plaintext $Y^{(3)}$. Since the computations are conducted in the clear, the later activation functions need not replacement. Finally, LaterNet outputs the prediction result l_{test} . The service provider proceed to compare the previously given true label l_{truth} with l_{test} , and returns an equality indicator 0 or 1. For a batch of test data, he would count the number of 1 indicator, and return a proportion of correct prediction. For the case using a posterior probability vector as a prediction output, we determine the indicator value according to the distance between the prediction output and the corresponding truth.

B. Correctness Proofs for the Splitting CNN Testing

Essentially, the correctness proofs will convince any future user that (1) the developer correctly runs PriorNet on the encrypted test data and returns the encrypted intermediate result as output; and (2) the service providers exactly take the intermediate result as input and correctly accomplish the successive computations of LaterNet, which produces a correct result. Moreover, we make two efforts to improve proving and verification costs, by reducing the number of multiplication gates and compressing multiple proofs, respectively.

Key idea. We start from a roadmap of QAPs-based zk-SNARKs as a high-level view shown in Fig. 4: firstly compiling the computations of our splitting CNN testing into circuits, then expressing the circuits as a set of QAPs, and lastly constructing the zk-SNARK proofs for the QAPs as well as generating commitments for linking together the zk-SNARK proofs which are constructed separately.

On top of the above roadmap, we make additional efforts for improvement: (a) We allow matrices in constructing the QAPs, leading to quadratic matrix programs (QMPs) [33], which is inspired by vCNN [11]'s efforts of applying polynomials into QAPs (QPPs, quadratic polynomial programs [41]). Our QMPs can optimize matrix multiplication relations, considering a convolution or full connection layer can be strategically represented by a single matrix multiplication operation. The operation of matrix multiplication then is compiled into the arithmetic circuits in QMPs with only a single multiplication gate. **As a consequence, the number**

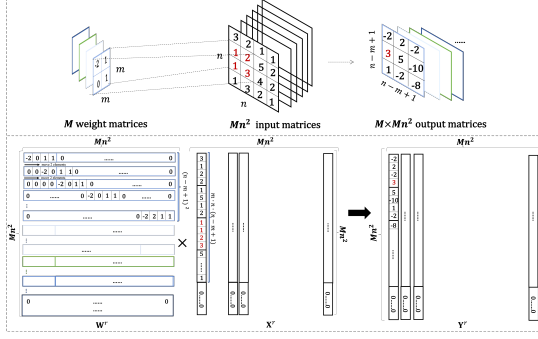


Fig. 5. Matrix multiplication for convolution operations.

of multiplication gates dominating proving costs is greatly reduced, compared to the previous case of using the original expression of QAPs. (b) We enable aggregating multiple proofs for different statements w.r.t test datasets over the same QAPs w.r.t the same CNN. The single proof after aggregation then is validated by a secure committee and the validity result based on the majority voting will be submitted and recorded on our public platform. *In such way, any future user only needs to check the validity result to determine whether or not the statements over the CNN are valid.*

(i) Optimizing matrix multiplication relations

As demonstrated in Fig. 5, we consider 2-D convolution operations between Mn^2 amount of $n \times n$ input matrices and $M > n$ amount of $m \times m$ convolution filters, which produces M^2n^2 filtered matrices of $(n - m + 1) \times (n - m + 1)$, via setting the stride 1. Specifically, by computing the inner products between each input matrix and each filter matrix, $\forall i, j \in [0, n - m]$ and $k \in [0, M - 1]$, it can be expressed as: $Y^k[i][j] = \sum_{l_r=0, l_c=0}^{m-1, m-1} X[i + l_r][j + l_c] \times W^k[l_r][l_c]$. Obviously, the multiplication complexity of such inner product computation is $O(n^2 \cdot m^2)$. Note that there are $M \cdot Mn^2$ amount of such set of Y , with respect to Mn^2 inputs and M filters. Thus, $O(M \cdot Mn^2 \cdot (n^2 \cdot m^2))$ multiplication gates in QAPs-based circuits are needed for handling Mn^2 inputs and M filters. Since proving time depends on the number of multiplication gates, a proof generation process for 2-D convolution operations becomes impractical.

Now, we seek for improving proving efficiency by reducing the number of multiplication gates. The very first step is to represent the inner products between the Mn^2 inputs and M filters with a *single matrix multiplication*. Concretely, we show a concrete example of the representation in Fig. 5. First, given Mn^2 amount of $n \times n$ input matrices $\{X\}$, they are reshaped into a square matrix X^r of $Mn^2 \times Mn^2$. Second, another square matrix W^r of the same dimension can be constructed by packing the M filter matrices in a moving and zero padding manner. As a result, the multiplication between the two square matrices produces a square matrix Y^r of $Mn^2 \times Mn^2$, which can also be regarded as a reshaped matrix from the original $M \cdot Mn^2$ amount of output matrices. Based on such representation, the two square matrices W^r and X^r of the matrix multiplication can later be the left and right inputs of an arithmetic circuit with only one multiplication gate. We proceed to express the above circuit with our new QMPs by using matrices in QAPs, which follows the similar principle

PriorNet prediction correctness.

$$\begin{aligned} R_{PN} &:= \{(\text{st}_{PN} = (C_{M_1,ed}, C_{X_{et}^{r(1)}}, Y_{et}^{r(3)}, ck_{PN}), \text{wt}_{PN} = (M_{1,ed}, X_{et}, r_{PN})) \mid \\ Y_{et}^{r(1)} &= W_{ed}^{r(1)} \odot X_{et}^{r(1)} \\ \wedge \{Y_{et}^{r(2)}[i][j] &= (Y_{et}^{r(1)}[i][j])^2 + Y_{et}^{r(1)}[i][j]\}_{i=0, j=0}^{Mn^2-1, Mn^2-1} \\ \wedge Y_{et}^{r(3)} &= f_{avg}(Y_{et}^{r(2)}) \\ \wedge C_{M_1,ed} &= \text{MPoly.Com}(M_{1,ed}, ck_{PN}, r_{PN}) \\ \wedge C_{X_{et}} &= \text{MPoly.Com}(X_{et}^{r(1)}, ck_{PN}, r_{PN}) \}. \\ //ck_{PN} &\text{ consists of the commitment keys.} \\ //r_{PN} &\text{ provides non-reused commitment randomnesses in Part 1.} \\ //C_{M_1,ed} &\text{ means the commitments to inputs, weights, intermediates of } M_1. \end{aligned}$$

LaterNet prediction correctness.

$$\begin{aligned} R_{LN} &:= \{(\text{st}_{LN} = (C_{Y^{r(3)}}^s, C_{M_2}, l_{test}, ck_{LN}), \text{wt}_{LN} = (Y^{r(3)}, M_2, r_{LN})) \mid \\ Y^{r(4)} &= W^{r(4)} \times Y^{r(3)} \wedge \{Y^{r(5)}[i][j] = \frac{1}{1 + e^{-Y^{r(4)}[i][j]}}\}_{i=0, j=0}^{Mn^2-1, Mn^2-1} \\ \wedge Y^{r(6)} &= f_{avg}(Y^{r(5)}) \wedge Y^{r(7)} = Y^{r(6)} \times W^{r(7)} \wedge Y^{r(8)} = Y^{r(7)} \times W^{r(8)} \\ \wedge l_{test}[j] &= \text{argmax}(Y^{r(8)}[j]) \\ \wedge C_{Y^{r(3)}}^s &= \text{MPoly.Com}(Y^{r(3)}, ck_{LN}, r_{LN}) \\ \wedge C_{M_2} &= \text{MPoly.Com}(M_2, ck_{LN}, r_{LN}) \}. \\ //C_{M_2} &\text{ represents the commitments to the weights and intermediates of } M_2. \end{aligned}$$

Fig. 6. Overview of relation definition.

of using polynomials in QAPs [41].

QMP definition [33]. For an arithmetic circuit with n_{in} input variables, n_{ot} output variables in $\mathbf{M}_{(F_p)}^{s \times s}$ and n_* multiplication gates, a QMP is consisting of three sets of polynomials $\{L_i(x), R_i(x), O_i(x)\}_{i=0}^m$ with coefficients in $\mathbf{M}_{(F_p)}^{s \times s}$ and a n_* -degree target polynomial $t(x) \in F_p[x]$. F_p is a large finite field, e.g., 2^{254} . The QMP computes the arithmetic circuit and $(A_0, \dots, A_{n_{in}}, A_{m-n_{ot}+1}, \dots, A_m) \in \mathbf{M}_{(F_p)}^{s \times s}$ is valid assignment for the $n_{in} + n_{ot}$ input/output variables *iff* there exists $m - n_{in} - n_{ot}$ coefficients $(A_{n_{in}+1}, \dots, A_{m-n_{ot}}) \in \mathbf{M}_{(F_p)}^{s \times s}$ for arbitrary $X \in \mathbf{M}_{(F_p)}^{s \times s}$ such that $t(x)$ divides $p(x, X) = \text{Tr}\{X^T \sum_{i=0}^m A_i L_i(x)\} \cdot \sum_{i=0}^m A_i R_i(x) - \text{Tr}\{X^T \sum_{i=0}^m A_i O_i(x)\}$. Herein, Tr means the trace of a square matrix, and the degree of the QMP is $\deg(t(x))$. We note that each wire of the arithmetic circuit is labeled by a square matrix $A_i \in \mathbf{M}_{(F_p)}^{s \times s}$. Suppose that the arithmetic circuit contains n_* multiplication gates, and then $t(x) = \prod_{r=0}^{n_*-1} t(x - x_r)$. With regard to a multiplication gate x_r , its left input wire is labeled by $\sum_{i=0}^m A_i L_i(x)$, right input wire is labeled by $\sum_{i=0}^m A_i R_i(x)$, and the output wire is $\sum_{i=0}^m A_i O_i(x)$. We note that the multiplication gate is constrained by $\text{Tr}\{X^T \sum_{i=0}^m A_i L_i(x)\} \cdot \sum_{i=0}^m A_i R_i(x) = \text{Tr}\{X^T \sum_{i=0}^m A_i O_i(x)\}$.

QMPs for matrix multiplication relations. As we introduced before, we can represent convolution operations as matrix multiplication $Y^r = W^r \times X^r$, where Y^r, X^r and $W^r \in \mathbf{M}_{(Z_p)}^{Mn^2 \times Mn^2}$. It is noteworthy that we can use advanced quantization techniques to transform floating-point numbers in the matrices into unsigned integer numbers in $[0, 255]$, and further adapt to large finite field. Now according to the QMP definition, when the matrix multiplication computation is expressed by the arithmetic circuit over matrices, the corresponding QMP is $\{L_W(x), R_X(x), O_Y(x), t(x)\}$ of the arithmetic circuit. Herein, there are three input/output variables, and the degree of the QMP is one.

Similarly, we can apply our above idea into full connection operations, and finally the operations can also be expressed with similarly low-degree QMPs.

(ii) Generating proofs for the splitting CNN testing

We here seek to elaborate a concrete procedure to generate

Part 1: Layer-wise prediction correctness for **PriorNet**.

Step 1: to prove that the prover knows the openings of the commitments in $\text{st}_{\text{PN}}^{S1}$

$$\begin{aligned} R_{\text{PN}}^{S1} := & \{ (\text{st}_{\text{PN}}^{S1} = (C_{L_1}, C_X, C_{\text{PN}}^{\text{inter}}, C_{L_1,k}, C_{L_2,k}, C_{L_3,k}, k, ck^{S1}, ck_{\text{PN}}), \text{wt}_{\text{PN}}^{S1} = (W_{ed}^{r(1)}, X_{et}^{r(1)}, Y_{et}^{r(1)}, Y_{et}^{r(2)}, Y_{et}^{r(3)}, W_{ed,k}^{r(1)}, X_{et,k}^{r(1)}, Y_{et,k}^{r(1)}, Y_{et,k}^{r(2)}, Y_{et,k}^{r(3)}, r_{\text{PN}}) \mid \\ & W_{ed,k}^{r(1)} = W_{ed}^{r(1)}(k) \wedge X_{et,k}^{r(1)} = X_{et}^{r(1)}(k) \wedge Y_{et,k}^{r(1)} = Y_{et}^{r(1)}(k) \wedge Y_{et,k}^{r(2)} = Y_{et}^{r(2)}(k) \wedge Y_{et,k}^{r(3)} = Y_{et}^{r(3)}(k) \\ & \wedge C_{L_1} = \text{MPoly.Com}(W_{ed}^{r(1)}, ck^{S1}, r_{\text{PN}}) \wedge C_X = \text{MPoly.Com}(X_{et}^{r(1)}, ck^{S1}, r_{\text{PN}}) \wedge C_{\text{PN}}^{\text{inter}} = \text{MPoly.Com}(Y_{et}^{r(1)}, Y_{et}^{r(2)}, Y_{et}^{r(3)}, ck_{\text{PN}}, r_{\text{PN}}) \\ & \wedge C_{L_1,k} = \text{MPoly.Com}(W_{ed,k}^{r(1)}, X_{et,k}^{r(1)}, Y_{et,k}^{r(1)}, Y_{et,k}^{r(2)}, Y_{et,k}^{r(3)}, ck_{\text{PN}}, r_{\text{PN}}) \wedge C_{L_2,k} = \text{MPoly.Com}(Y_{et,k}^{r(2)}, Y_{et,k}^{r(3)}, ck_{\text{PN}}, r_{\text{PN}}) \wedge C_{L_3,k} = \text{MPoly.Com}(Y_{et,k}^{r(3)}, ck_{\text{PN}}, r_{\text{PN}}) \}. \\ & //ck_{\text{PN}} \text{ is the commitment key used before the evaluation while } ck^{S1} \text{ is used during the prediction} \\ & //C_X \text{ commits to } X_{et}^{r(1)} \text{ whose compression version, e.g., hash of it, is submitted to the public platform before} \\ & //C_{L_1} \text{ commits to the same } W_{ed}^{r(1)} \text{ that has been committed by model owner in advance} \end{aligned}$$

Step 2: to prove that the equations with respect to L_1, L_2, L_3 hold

$$\begin{aligned} R_{\text{PN}}^{S2}[L_1] := & \{ (\text{st}_{\text{PN}}^{S2} = (C'_{L_1,k}, k, ck_{L_1}), \text{wt}_{\text{PN}}^{S2} = (W_{ed,k}^{r(1)}, X_{et,k}^{r(1)}, Y_{et,k}^{r(1)}, r_{\text{PN}})) \mid Y_{et,k}^{r(1)} = W_{ed,k}^{r(1)} \odot X_{et,k}^{r(1)} \wedge C'_{L_1,k} = \text{MPoly.Com}(W_{ed,k}^{r(1)}, X_{et,k}^{r(1)}, Y_{et,k}^{r(1)}, ck_{L_1}, r_{\text{PN}}) \}. \\ & //ck_{L_1} \text{ is built depending on the relation; } C'_{L_1,k} \text{ commits to the consistent } W_{ed,k}^{r(1)}, X_{et,k}^{r(1)}, Y_{et,k}^{r(1)} \text{ with the above } C_{L_1,k} \\ R_{\text{PN}}^{S2}[L_2, L_3] := & \{ (\text{st}_{\text{PN}}^{S2} = (C'_{L_2,k}, C_{L_2}[Y_{et,k}^{r(2)}], C'_{L_3,k}, C_{L_3}[Y_{et,k}^{r(2)}], k, ck_{L_2}, ck_{L_3}), \text{wt}_{\text{PN}}^{S2} = (Y_{et,k}^{r(2)}, Y_{et,k}^{r(3)}, r_{\text{PN}}) \mid \\ & \{ Y_{et,k}^{r(2)}[i][j] = (Y_{et,k}^{r(1)}[i][j])^2 + Y_{et,k}^{r(1)}[i][j] \}_{i=0,j=0}^{Mn^2-1, Mn^2-1} \wedge Y_{et,k}^{r(3)} = f^{\text{avg}}(Y_{et,k}^{r(2)}) \wedge C'_{L_2,k} = \text{MPoly.Com}(Y_{et,k}^{r(2)}, ck_{L_2}, r_{\text{PN}}) \\ & \wedge C_{L_2}[Y_{et,k}^{r(2)}] = \text{MPoly.Com}(Y_{et,k}^{r(2)}, ck_{L_2}, r_{\text{PN}}) \wedge C'_{L_3,k} = \text{MPoly.Com}(Y_{et,k}^{r(3)}, ck_{L_3}, r_{\text{PN}}) \wedge C_{L_3}[Y_{et,k}^{r(2)}] = \text{MPoly.Com}(Y_{et,k}^{r(2)}, ck_{L_3}, r_{\text{PN}}) \}. \\ & //C'_{L_2,k} \text{ (and } C'_{L_3,k}) \text{ commit to the same } Y_{et,k}^{r(2)} \text{ (resp. } Y_{et,k}^{r(3)}) \text{ with } C_{L_2,k} \text{ (resp. } C_{L_3,k}) \\ & //C_{L_2}[Y_{et,k}^{r(2)}] \text{ should commit to the same } Y_{et,k}^{r(2)} \text{ that } C'_{L_1,k} \text{ commits to; similarly, } C_{L_3}[Y_{et,k}^{r(2)}] \text{ should commit to the same } Y_{et,k}^{r(2)} \text{ that } C'_{L_2,k} \text{ commits to} \end{aligned}$$

Part 2: Layer-wise prediction correctness for **LaterNet**.

$$\begin{aligned} R_{\text{LN}}[L_4] := & \{ (\text{st}_{\text{LN}} = (C_{Y^{r(3)}}, C_{L_4}, C_{Y^{r(4)}}, ck_{L_4}), \text{wt}_{\text{LN}} = (W^{r(4)}, Y^{r(3)}, Y^{r(4)}, r_{\text{LN}})) \mid Y^{r(4)} = W^{r(4)} \times Y^{r(3)} \\ & \wedge C_{Y^{r(3)}} = \text{MPoly.Com}(Y^{r(3)}, ck_{L_4}, r_{\text{LN}}) \wedge C_{L_4} = \text{MPoly.Com}(W^{r(4)}, ck_{L_4}, r_{\text{LN}}) \wedge C_{Y^{r(4)}} = \text{MPoly.Com}(Y^{r(4)}, ck_{L_4}, r_{\text{LN}}) \}. \\ & //C_{Y^{r(3)}} \text{ should commit to } Y^{r(3)} \text{ whose encryption is committed in } C_{\text{PN}}^{\text{inter}} \\ R_{\text{LN}}[L_5, L_6] := & \{ (\text{st}_{\text{LN}} = (C_{L_5}[Y^{r(4)}], C_{Y^{r(5)}}, C_{L_6}[Y^{r(5)}], C_{Y^{r(6)}}, ck_{L_5}, ck_{L_6}), \text{wt}_{\text{LN}} = (Y^{r(4)}, Y^{r(5)}, Y^{r(6)}, r_{\text{LN}})) \mid \\ & \{ Y^{r(5)}[i][j] = \frac{1}{1+e^{-Y^{r(4)}[i][j]}} \}_{i=0,j=0}^{Mn^2-1, Mn^2-1} \wedge Y^{r(6)} = f^{\text{avg}}(Y^{r(5)}) \wedge C_{L_5}[Y^{r(4)}] = \text{MPoly.Com}(Y^{r(4)}, ck_{L_5}, r_{\text{LN}}) \wedge C_{Y^{r(5)}} = \text{MPoly.Com}(Y^{r(5)}, ck_{L_6}, r_{\text{LN}}) \\ & \wedge C_{L_6}[Y^{r(5)}] = \text{MPoly.Com}(Y^{r(5)}, ck_{L_6}, r_{\text{LN}}) \wedge C_{Y^{r(6)}} = \text{MPoly.Com}(Y^{r(6)}, ck_{L_6}, r_{\text{LN}}) \}. \\ & //C_{L_5}[Y^{r(4)}] \text{ should commit to } Y^{r(4)} \text{ that is committed in } C_{Y^{r(4)}} \text{ of } L_4 \\ & //C_{L_6}[Y^{r(5)}] \text{ should commit to } Y^{r(5)} \text{ that is committed in } C_{Y^{r(5)}} \text{ of } L_5 \\ R_{\text{LN}}[L_7, L_8] := & \{ (\text{st}_{\text{LN}} = (C_{L_7}, C_{L_7}[Y^{r(6)}], C_{L_8}[Y^{r(8)}], ck_{L_7}, ck_{L_8}), \text{wt}_{\text{LN}} = (W^{r(7)}, W^{r(8)}, Y^{r(6)}, Y^{r(7)}, Y^{r(8)}, r_{\text{LN}})) \mid Y^{r(7)} = Y^{r(6)} \times W^{r(7)} \\ & \wedge C_{L_7} = \text{MPoly.Com}(W^{r(7)}, W^{r(8)}, ck_{L_7}, r_{\text{LN}}) \wedge C_{L_7}[Y^{r(6)}] = \text{MPoly.Com}(Y^{r(6)}, ck_{L_7}, r_{\text{LN}}) \wedge C_{L_8}[Y^{r(8)}] = \text{MPoly.Com}(Y^{r(8)}, ck_{L_8}, r_{\text{LN}}) \}. \\ & //C_{L_7}[Y^{r(6)}] \text{ should commit to } Y^{r(6)} \text{ that is committed in } C_{Y^{r(6)}} \text{ of } L_6 \\ R_{\text{LN}}[L_o] := & \{ (\text{st}_{\text{LN}} = (C_{L_o}[Y^{r(8)}], I_{\text{test}}, ck_{L_o}), \text{wt}_{\text{LN}} = (Y^{r(8)})) \mid I_{\text{test}}[j] = \text{argmax}(Y^{r(8)}[j]) \wedge C_{L_o}[Y^{r(8)}] = \text{MPoly.Com}(Y^{r(8)}, ck_{L_o}, r_{\text{LN}}) \}. \\ & //C_{L_o}[Y^{r(8)}] \text{ should commit to } Y^{r(8)} \text{ that is committed in } C_{Y^{r(8)}} \text{ of } L_8 \end{aligned}$$

Fig. 7. Layer-by-layer relation definition for our splitting CNN testing.

correctness proofs based on CaP zk-SNARKs. We begin with relation definition, and then present concrete realization for correctness proof generation.

Relation definition. As elaborated in Fig. 6, from the top to the bottom, we first define relations R_{PN} and R_{LN} to be proved with regard to PriorNet and LaterNet execution correctness. Then, we further denote more detailed relations for proving R_{PN} and R_{LN} accordingly in a layer-by-layer manner in Fig. 7. Lastly, we also denote the relations in Appendix D for proving that all layers are sequentially connected consistently.

At a high level, we need to prove that PriorNet and LaterNet are executed correctly *iff* both of binary relations R_{PN} and R_{LN} return 1, which means R_{PN} and R_{LN} hold on the corresponding pairs of (st, wt) . For R_{PN} , we generate publicly verifiable proofs for convincing that $Y_{et}^{r(3)}$ is computed correctly in an encryption manner, with the trained parameters of PriorNet $\mathbf{M}_{1,ed}$ and encrypted test inputs $X_{et}^{r(1)}$ through the following sequential equations: $Y_{et}^{r(1)} = W_{ed}^{r(1)} \odot X_{et}^{r(1)}$, $\{Y_{et}^{r(2)}[i][j] = (Y_{et}^{r(1)}[i][j])^2\}_{i=0,j=0}^{Mn^2-1, Mn^2-1}$, and $Y_{et}^{r(3)} = f^{\text{avg}}(Y_{et}^{r(2)})$. Here, witnesses $\mathbf{M}_{1,ed}$ and $X_{et}^{r(1)}$ are committed with the commit key ck_{PN} , and the generated commitments plus $Y_{et}^{r(3)}$ are public as the statement to be proved. For R_{LN} , we generate proofs to convince any verifier that LaterNet takes the correct plaintext $Y^{r(3)}$ and returns the correct plaintext I_{test} by conducting the sequential operations including $Y^{r(4)} = W^{r(4)} \times Y^{r(3)}$, $\{Y^{r(5)}[i][j] = \frac{1}{1+e^{-Y^{r(4)}[i][j]}}\}_{i=0,j=0}^{Mn^2-1, Mn^2-1}$,

$$Y^{r(6)} = f^{\text{avg}}(Y^{r(5)}), Y^{r(7)} = Y^{r(6)} \times W^{r(7)}, Y^{r(8)} = Y^{r(7)} \times W^{r(8)}, I_{\text{test}}[j] = \text{argmax}(Y^{r(8)}[j]).$$

The processes of proof generation for R_{PN} and R_{LN} are conducted separately, since the two parts PriorNet and LaterNet are executed by different entities. Furthermore, due to the nature of layer-wise prediction over different computations, correctness proofs for each layer are produced separately. Hence, we proceed to define detailed relations with respect to the execution correctness of each layer in Fig. 7. With respect to Fig. 4, they are $R_{\text{PN}}^{S1}, R_{\text{PN}}^{S2}[L_1]$ (resp. proof π_{PN}^1), $R_{\text{PN}}^{S2}[L_2, L_3]$ (resp. proof π_{PN}^2), $R_{\text{LN}}^{S2}[L_4]$ (resp. proof π_{LN}^1), $R_{\text{LN}}^{S2}[L_5, L_6]$ (resp. proof π_{LN}^2), $R_{\text{LN}}^{S2}[L_7, L_8]$ (resp. proof π_{LN}^3) and $R_{\text{LN}}^{S2}[L_o]$ (resp. proof π_{LN}^4). Besides, in order to prove that the sequential computations use the consistent intermediates, we additionally define the relations like $R_{L_{1,2}}$ in Appendix D, for later linking together the separately generated proofs, so as to realize the interoperability between the proofs.

Separate proofs generation. We can generate correctness proofs for the above detailed relations, with respect to each part and each layer. The first part is proving R_{PN} , and the second part is proving R_{LN} . In relation R_{PN} , we define that PriorNet is performed in an encryption manner, by taking the encrypted inputs $X_{et}^{r(1)}$ in ring field $Z_q[x](x^{d_c} + 1)$, while in relation R_{LN} , LaterNet performs in plaintext. For ease of reading, we next only present the concrete procedure to generate correctness proofs for the first convolution layer L_1 in the first part, since the proofs for the second part can be generated

Step 1 CaP zk-SNARK Proofs of Knowledge of Commitments
1: $\text{MUniEv-II.Setup}(\lambda, d_c, n_c) \rightarrow \text{ck}^{S1}$; 2: $//d_c$ refers to the degree of ciphers; n_c is the number of ciphers 3: $g, h \xleftarrow{\$} G, g^* \xleftarrow{\$} G, \alpha, s, t \xleftarrow{\$} Z_p$ 4: $\hat{g} = g^\alpha, \hat{h} = h^\alpha, \hat{g}^* = g^{*\alpha}, \hat{g}_1^* = g^{*s}, h_1 = h^s$, 5: $\{g_{i,j} = g^{s^{i,j}}, \hat{g}_{i,j} = \hat{g}^{s^{i,j}}\}_{i=0,j=0}^{d_c, n_c}$, HASH: $G^* \times Z_q^* \rightarrow Z_p$ 6: $\text{ck}^{S1} := (g, h, g^*, \{g_{i,j}, \hat{g}_{i,j}\}_{i=0,j=0}^{d_c, n_c}, \hat{g}, \hat{h}, \hat{g}^*, \hat{g}_1^*, h_1, \text{HASH})$ 7: $\text{MUniEv-II.Prove}(\text{ck}^{S1}, \mathbf{W}_{ed}^{r(1)}, \mathbf{X}_{et}^{r(1)}) \rightarrow \pi^{S1}$; 8: $//\mathbf{W}_{ed}^{r(1)}, \mathbf{X}_{et}^{r(1)}$ are square matrices of $l_{\text{new}} = Mn^2$ 9: $//l_{\text{new}}^2$ is smaller than n_c 10: $//\text{call the commitment scheme MPoly.Com}$ 11: call $\text{MPoly.Com}(\text{ck}^{S1}, \mathbf{W}_{ed}^{r(1)}) \rightarrow C_{W1}$: $- r_{W1} \xleftarrow{\$} Z_p$, $- C_{W1}^1 = h^{r_{W1}} \prod_{i=0,j=0}^{d_c, l_{\text{new}}^2-1} w_{i,j}, C_{W1}^2 = \hat{h}^{r_{W1}} \prod_{i=0,j=0}^{d_c, l_{\text{new}}^2-1} w_{i,j}$, $- C_{W1} := (C_{W1}^1, C_{W1}^2)$ 12: call $\text{MPoly.Com}(\text{ck}^{S1}, \mathbf{X}_{et}^{r(1)}) \rightarrow C_X$: $- r_X \xleftarrow{\$} Z_p, C_X^1 = h^{r_X} \prod_{i=0,j=0}^{d_c, l_{\text{new}}^2-1} x_{i,j}, C_X^2 = \hat{h}^{r_X} \prod_{i=0,j=0}^{d_c, l_{\text{new}}^2-1} x_{i,j}$, $- C_X := (C_X^1, C_X^2)$ 13: call $\text{MPoly.Com}(\text{ck}^{S1}, \mathbf{Y}_{et}^{r(1)}) \rightarrow C_Y$: $- r_Y \xleftarrow{\$} Z_p, C_Y^1 = h^{r_Y} \prod_{i=0,j=0}^{d_c, l_{\text{new}}^2-1} y_{i,j}, C_Y^2 = \hat{h}^{r_Y} \prod_{i=0,j=0}^{d_c, l_{\text{new}}^2-1} y_{i,j}$, $- C_Y := (C_Y^1, C_Y^2)$ 14: $k = \text{HASH}(C_{W1}, C_X, \mathbf{W}_{ed}^{r(1)}, \mathbf{X}_{et}^{r(1)}, \mathbf{Y}_{et}^{r(1)})$ 15: $//\mathbf{X}_{et}^{r(1)} \in \mathbf{M}_{Z_q[x](x^{d_c+1})}^{l_{\text{new}}^2}, \mathbf{X}(x, y) = \sum_{i=0,j=0}^{d_c, l_{\text{new}}^2-1} x_{i,j} x^i y^j$ 16: $//\mathbf{W}_{ed}^{r(1)} \in \mathbf{M}_{Z_q[x](x^{d_c+1})}^{l_{\text{new}}^2}, \mathbf{W}(x, y) = \sum_{i=0,j=0}^{d_c, l_{\text{new}}^2-1} w_{i,j} x^i y^j$ 17: $//\mathbf{Y}_{et}^{r(1)} \in \mathbf{M}_{Z_q[x](x^{d_c+1})}^{l_{\text{new}}^2}, \mathbf{Y}(x, y) = \sum_{i=0,j=0}^{d_c, l_{\text{new}}^2-1} y_{i,j} x^i y^j$ 18: $L_1 := L_1(x, y) = \mathbf{W}(x, y) + \mathbf{X}(x, y) + \mathbf{Y}(x, y) = \sum_{i=0,j=0}^{d_c, l_{\text{new}}^2-1} l_{i,j} x^i y^j$ 19: call $\text{MPoly.Com}(\text{ck}^{S1}, L_1(s, t)) \rightarrow C_{L1} = (C_{L1}^1, C_{L1}^2)$ 20: $L_{1,k} := L_1(k, y) = \mathbf{W}(k, y) + \mathbf{X}(k, y) + \mathbf{Y}(k, y) = \sum_{i=0,j=0}^{d_c, l_{\text{new}}^2-1} l_{i,j} k^i y^j$ 21: call $\text{MPoly.Com}(\text{ck}^{S1}, \mathbf{W}_{ed,k}^{r(1)}) \rightarrow C_{w,k} = (C_{w,k}^1, C_{w,k}^2)$ 22: call $\text{MPoly.Com}(\text{ck}^{S1}, \mathbf{X}_{et,k}^{r(1)}) \rightarrow C_{x,k} = (C_{x,k}^1, C_{x,k}^2)$ 23: call $\text{MPoly.Com}(\text{ck}^{S1}, \mathbf{Y}_{et,k}^{r(1)}) \rightarrow C_{y,k} = (C_{y,k}^1, C_{y,k}^2)$ 24: $C_{L1,k}^1 = (C_{w,k}^1 \cdot C_{x,k}^1 \cdot C_{y,k}^1)$; $C_{L1,k}^2 = (C_{w,k}^2 \cdot C_{x,k}^2 \cdot C_{y,k}^2)$ 25: $T(x, y) = \frac{L_1(x, y) - L_1(k, y)}{(x-k)}$ 26: $\bar{g} = \frac{h_1}{h^k}, a, b \xleftarrow{\$} Z_p$, 27: call $\text{MPoly.Com}(\text{ck}^{S1}, T(x, y)) \rightarrow C_T$: $- r_T \xleftarrow{\$} Z_p, C_T^1 = h^{r_T} \prod_{t=0,i=0,j=0}^{d_c-1, d_c-t, l_{\text{new}}^2-1} l_{i+t,j} k^{i-1} s^i t^j$, $- C_T^1 = h^{r_T} \prod_{t=0,i=0,j=0}^{d_c-1, d_c-t, l_{\text{new}}^2-1} l_{i+t,j} k^{i-1} s^i t^j$, $- C_T := (C_T^1, C_T^2)$ 28: $U = e(h^a \bar{g}^b, g^*)$, $e \leftarrow \text{HASH}(C_{L1}, C_{L1,k}, C_T, U, k)$, 29: $\sigma = a - (r_{L1,k} - r_{L1}) \cdot e \bmod q, \tau = b - r_T \cdot e \bmod q, \pi^{S1} = (C_T, e, \sigma, \tau)$ 30: $\text{MUniEv-II.Verify}(\text{ck}^{S1}, C_{L1}, C_X, C_{L1,k}, C_T, k, \pi^{S1}) \rightarrow 0/1$: 31: $b_1 := (e(C_{L1}^1, \hat{g}^*) == e(C_{L1}^2, g^*))$; $b_2 := (e(C_X^1, \hat{g}^*) == e(C_X^2, g^*))$; 32: $b_3 := (e(C_{w,k}^1, \hat{g}^*) == e(C_{w,k}^2, g^*) \wedge e(C_{x,k}^1, \hat{g}^*) == e(C_{x,k}^2, g^*)$ $\wedge e(C_{y,k}^1, \hat{g}^*) == e(C_{y,k}^2, g^*))$; 33: $b_4 := (e(C_T^1, \hat{g}^*) == e(C_T^2, g^*))$; 34: $H = e(C_T^1, g^{*k} / g^{*k}) \cdot e(C_{L1}^1 / C_{L1,k}^1, g^*)^{-1}, \bar{g} = h_1 / h^k$, 35: $U = e(h^\sigma \bar{g}^\tau, g^*) \cdot H^e$, 36: $b_5 := (e == \text{HASH}(C_{L1}, C_{L1,k}, C_T, U, k))$; 37: $b = (b_1 \wedge b_2 \wedge b_3 \wedge b_4 \wedge b_5) \rightarrow 0/1$.

Fig. 8. Generating zk-SNARK proofs for relation R_{PN}^{S1} .

similar to Step 2 for the first part (will be introduced later).

Specifically, we adopt the methodology of efficient verification computation on encrypted data recently proposed by Fiore *et al* [21]. Then, we integrate it with the aforementioned CaP zk-SNARK from Groth scheme for proving the satisfiability of QMP-based arithmetic circuits. As a result, we generate our proofs for PriorNet prediction correctness with two steps, and we specially focus on the first layer of PriorNet. As demonstrated in Fig. 8, Step 1 is to prove the knowledge

Step 2 CaP zk-SNARK Proofs over QMP
$//\text{st} = (\mathbf{W}_{ed,k}^{r(1)}, \mathbf{X}_{et,k}^{r(1)}, \mathbf{Y}_{et,k}^{r(1)}); \text{io} = m = 3; \text{QMP} = (L(x), R(x), O(x), t(x))$ $//p(x, \mathbf{Z}) = \text{Tr}\{\mathbf{Z}^T \cdot L(x) \cdot R(x)\} - \text{Tr}\{\mathbf{Z}^T \cdot O(x)\} = h(x, \mathbf{Z})t(x), \forall \mathbf{Z} \in \mathbf{M}_{(Z_p)}^{l_{\text{new}}^2}$ 1: AC-II.Setup($1^\lambda, \text{QMP}$) \rightarrow crs: 2: $(\alpha, \beta, \gamma, \delta, \eta, z) \leftarrow Z_p, \mathbf{Z} \leftarrow \mathbf{M}_{(Z_p)}^{l_{\text{new}}^2}, g, h \leftarrow G$ 3: $\text{crs} := (g, h, g^\alpha, g^\beta, h^\beta, h^\gamma, g^\delta, h^\delta, g^{\frac{\eta}{\delta}}, g^{\frac{\eta}{\gamma}}, \{\text{OP}_i = g^{\frac{\beta L_i(z)}{\gamma}} \cdot g^{\frac{\alpha R_i(z)}{\gamma}} \cdot g^{\frac{O_i(z)}{\gamma}}\}_{i=0}^t)$ 4: AC-II.Prove(crs, st, wt) $\rightarrow \pi^{S2}$: 5: $L(x) = \mathbf{W}_{ed,k}^{r(1)} \cdot L_{\mathbf{W}}(z); R(x) = \mathbf{X}_{et,k}^{r(1)} \cdot R_{\mathbf{X}}(z); O(x) = \mathbf{Y}_{et,k}^{r(1)} \cdot O_{\mathbf{Y}}(z)$ 6: $(t, s, v) \xleftarrow{\$} Z_p, A := g^\alpha \cdot g^{Z^T L(z)} \cdot g^{\delta t}, B := h^\beta \cdot h^{R(z)} \cdot h^{\delta s}$, 7: $C := g^{h(z, Z)t(z)/\delta} \cdot A^s \cdot (g^\beta \cdot g^{R(z)} \cdot g^{\delta s})^t \cdot g^{-ts\delta} \cdot g^{-v\eta/\delta}$, $D := g^{\frac{\beta Z^T L(z)}{\gamma}} \cdot g^{\frac{\alpha R(z)}{\gamma}} \cdot g^{\frac{Z^T O(z)}{\gamma}} \cdot g^{v\eta/\gamma}$, 8: $d_1 = g^{\frac{\beta L(z)}{\gamma}} \cdot g^{v\eta/\gamma}, d_2 = g^{\frac{\alpha R(z)}{\gamma}} \cdot g^{v\eta/\gamma}, d_3 = g^{\frac{O(z)}{\gamma}} \cdot g^{v\eta/\gamma}$, 9: $C_{L1,k} := (d_1, d_2, d_3), \pi_{L1,k}^{S2} := (A, B, C, D, C_{L1,k})$ 10: AC-II.Verify(crs, $\pi_{L1,k}^{S2}$) $\rightarrow 0/1$: 11: $b := (\text{Tr}\{e(A, B)\} == \text{Tr}\{e(g^\alpha, h^\beta) \cdot e(D, h^\gamma) \cdot e(C, h^\delta)\}) \rightarrow 0/1$.

Fig. 9. Generating zk-SNARK proofs for relation $R_{PN}^{S2}[L_1]$.

of commitments to test inputs, trained weights of L_1 , and intermediate outputs, by proving simultaneous evaluation of multiple ring field polynomials on a same point. Step 2 shown in Fig. 9 is to prove the arithmetic correctness of the matrix multiplication computation by following our idea of QMPs.

Let us see more details about the commitment generation in the above steps, which is essential to enable the interoperability between the separate proofs. Herein, the interoperability between the separate proofs are two-fold: (i1) linking π^{S1} with π^{S2} ; (i2) linking π^{S2} with the proof for relation $R_{PN}^{S2}[L_2, L_3]$. In particular, (i1) requires that $C_{L1,k}^1$ (see line 18 to 24 in Fig. 8) and $C_{L1,k}'$ (see line 9 in Fig. 9) open to the same $\mathbf{W}_{ed,k}^{r(1)}, \mathbf{X}_{ed,k}^{r(1)}$ and $\mathbf{Y}_{ed,k}^{r(1)}$. (i2) requires that $C_{L2}[\mathbf{Y}_{ed,k}^{r(1)}]$ commits to the consistent $\mathbf{Y}_{ed,k}^{r(1)}$ which is committed to in $C_{L1,k}'$.

CP _{link} proof for R_{PN}^{link}
1: build $\mathbf{R}_{PN}^{\text{link}} := \{(\text{st}_{PN}^{\text{link}}, \mathbf{w}_{PN}^{\text{link}}) \mid \mathbf{R}_{\mathbf{W}} \wedge \mathbf{R}_{\mathbf{X}} \wedge \mathbf{R}_{\mathbf{Y}}\}$ 2: $\text{CP}_{\text{link}}.\text{Setup}(1^\lambda, \text{ck}_{PN}, \mathbf{R}_{PN}^{\text{link}}) \rightarrow \text{crs}^{\text{link}}$: 3: build ck from $\text{ck}_{PN}, \text{ck}_{L1}$ 4: call $\prod_{as}.\text{Setup}(\text{ck}) \rightarrow \text{crs}^{\text{link}}$ 5: $\text{CP}_{\text{link}}.\text{Prove}(\text{crs}^{\text{link}}, C_{L1,k}^1, C_{L1,k}', \mathbf{r}_{PN}, \mathbf{W}_{ed,k}^{r(1)}, \mathbf{X}_{et,k}^{r(1)}, \mathbf{Y}_{et,k}^{r(1)}) \rightarrow \pi^{\text{link}}$: 6: build \mathbf{C} from $C_{L1,k}^1, C_{L1,k}'$ 7: build \mathbf{wt} from $\mathbf{r}_{PN}, \mathbf{W}_{ed,k}^{r(1)}, \mathbf{X}_{et,k}^{r(1)}, \mathbf{Y}_{et,k}^{r(1)}$ 8: call $\prod_{as}.\text{Prove}(\text{crs}^{\text{link}}, \mathbf{C}, \mathbf{wt}) \rightarrow \text{crs}^{\text{link}}$ 9: $\text{CP}_{\text{link}}.\text{Verify}(\text{crs}^{\text{link}}, C_{L1,k}^1, C_{L1,k}') \rightarrow \pi^{\text{link}}$: 10: call $\prod_{as}.\text{Verify}(\text{crs}^{\text{link}}, \mathbf{C}) \rightarrow \pi^{\text{link}}$

Fig. 10. Generating zk-SNARK proofs for relation R_{PN}^{link} .

Separate proofs composition. To ensure the aforementioned interoperability between separate proofs, we now need to prove the relation that two commitments open to the same values. Note that the commitments $C_{L1,k}^1, C_{L1,k}'$ and $C_{L2}[\mathbf{Y}_{ed,k}^{r(1)}]$ are Pedersen-like commitments. We make use of the previously proposed CaP zk-SNARK CP_{link} [20] to composite two separate proofs, *e.g.* π^{S1} and π_{L1}^{S2} , via proving relation R_{PN}^{link} , as denoted in Appendix D. Also, the similar methodology can be applied into the relation $R_{L1,2}$. The key idea is to reshape the computation of Pedersen commitment into the linear subspace computation. Concretely, the relation of proving $C_{w,k}^1$ and d_1 committing to $\mathbf{W}_{ed,k}^{r(1)}$ is transformed

into the linear subspace relation R_W [20] is shown in Fig. 15 in Appendix C, where how we build C , ck and wt .

Similarly, we can deduce relations R_X and R_Y for proving $C_{x,k}^1$ and d_2 committing to $X_{et,k}^{r(1)}$, and $C_{y,k}^1$ and d_3 committing to $Y_{et,k}^{r(1)}$, respectively. As a result, we represent the former R_{PN}^{link} as $R_{PN}^{link} := \{(st_{PN}^{link}, wt_{PN}^{link}) \mid R_W \wedge R_X \wedge R_Y\}$. Then, as demonstrated in Fig. 10, the proof π^{link} for such a relation is generated by leveraging CP_{link} that calls a scheme for proving linear subspace relations R_W , R_X and R_Y .

(iii) Aggregating multiple proofs

We consider that a CNN is tested with the test data from multiple testers, and there are hence multiple proofs with respect to proving the correctness of each inference process. For ease of storage overhead and verification cost, it is desirable to aggregate multiple proofs into a single proof. Specifically, storing the multiple proofs on the blockchain is naturally not satisfactory due to high cost, *e.g.* gas cost. Besides, ensuring the verification computation as simple and low as possible can make our public platform more easily accessible to a later-coming user. To the end, this section proceeds to introduce the algorithm of aggregating multiple proofs w.r.t an identical model but different statements based on different test data.

Relation definition. Suppose there are n_t CaP proofs $\{\pi^{m,i} = (A_i, B_i, C_i, D_i)\}_{i \in [n_t]}$ w.r.t a CNN m which is tested by n_t testers. We define the aggregation relation that the multiple generated proofs are valid at the same time: $R_{agg} = \{(st_{agg}, wt_{agg}) \mid \{AC- \prod_i . Verify(vk^m, \pi^{m,i}, st^{m,i}) \rightarrow 1\}_{i \in [n_t]}\}$. Here, vk^m is the verification key, extracted from the common randomness string in the Setup algorithm, and $vk^m = (g^\alpha, h^\beta, \{OP_i\}_{i=0}^t, h^\gamma, h^\delta)$. We note that vk^m is the same for the different statements $\{st^{m,i}\}_{i \in [n_t]}$, each of which contains $st^{m,i} = (a_{i,0}, \dots, a_{i,t})$. $\pi^{m,i}$ is the proof for the statement $st^{m,i}$ based on the different test data and the different intermediates during the computation of m .

Proof aggregation. With the defined relation, we are ready to provide a proof for it. A crucial tool to generate such a proof is recently proposed SnarkPack [34]. The external effort for us is to extend this work targeted at the original Groth16 scheme [18] without a commit-and-prove component to our case, that is, the proofs based on the CaP Groth16 scheme [20] as well as our QMPs-based proofs (see Fig. 9). As shown in line 18 of Fig. 11, we additionally compute a multi-exponentiation inner product for $\{D_i\}_{i \in [n_t]}$ of the multiple proofs, which is similar to computing the original $\{C_i\}_{i \in [n_t]}$. As a result, we enable a single verification on the aggregated proof π_{agg} for a later-coming user who is interested in the model m that is tested by n_t testers.

V. SECURITY ANALYSIS

This section analyses that our publicly verifiable evaluation method for a separate CNN testing which is built with the CaP zk-SNARKs and Leveled FHE satisfies correctness, security and privacy.

Theorem 1. *If the underlying CaP zk-SNARKs are secure commit-and-prove arguments of knowledge \prod_s , the used leveled FHE scheme L-FHE is semantically secure and commit-*

Aggregating multiple CaP proofs	
1: SnarkPack.Setup($1^\lambda, R_{agg}$) \rightarrow crs_{agg} :	
2: obtain g and h from crs ; $a, b \xleftarrow{\$} Z_p$	
3: generate commitment keys ck_{two} and ck_{one} :	
4: $\vec{v}_1 = (h, h^a, \dots, h^{a^{n-1}})$, $\vec{w}_1 = (g^{a^n}, \dots, g^{a^{2n-1}})$,	
5: $\vec{v}_2 = (h, h^b, \dots, h^{b^{n-1}})$, $\vec{w}_2 = (g^{b^n}, \dots, g^{b^{2n-1}})$	
6: $ck_{two} = (\vec{v}_1, \vec{v}_2, \vec{w}_1, \vec{w}_2)$, $ck_{one} = (\vec{v}_1, \vec{v}_2)$	
//call a generalized inner product argument MT_IPP (see Section 5.2 of [34])	
7: MT_IPP.Setup($1^\lambda, R_{MT}$) \rightarrow crs_{MT}	
8: $crs_{agg} = (vk^m, ck_{two}, ck_{one}, crs_{MT})$	
9: SnarkPack.Prove($crs_{agg}, \{st^{m,i}\}_{i \in [n_t]}, \{\pi^{m,i}\}_{i \in [n_t]}\}$:	
10: //commit to $\{A_i\}_{i \in [n_t]}$ and $\{B_i\}_{i \in [n_t]}$ using ck_{two}	
11: $C_{1-AB} = e(A_0, h) \dots e(A_{n_t-1}, h^{a^{n-1}}) \dots e(g^{a^n}, B_0) \dots e(g^{a^{2n-1}}, B_{n_t-1})$	
12: $C_{2-AB} = e(A_0, h) \dots e(B_{n_t-1}, h^{b^{n-1}}) \dots e(g^{b^n}, B_0) \dots e(g^{b^{2n-1}}, B_{n_t-1})$	
13: //commit to $\{C_i\}_{i \in [n_t]}$ and $\{D_i\}_{i \in [n_t]}$ separately using ck_{one}	
14: $C_C = e(C_0, h) \dots e(C_{n_t-1}, h^{a^{n-1}})$, $C_C = e(C_0, h) \dots e(C_{n_t-1}, h^{b^{n-1}})$	
15: $C_D = e(D_0, h) \dots e(D_{n_t-1}, h^{a^{n-1}})$, $C_D = e(D_0, h) \dots e(D_{n_t-1}, h^{b^{n-1}})$	
16: //generate a challenge	
17: $r = \text{Hash}(\{st^{m,i}\}_{i \in [n_t]}, C_{1-AB}, C_{2-AB}, C_C, C_D)$, $\vec{r} = (r^0, \dots, r^{n_t-1})$	
18: $I_{AB} = \prod_{i=0}^{n_t-1} e(A_i, B_i)^{r^i}$, $I_C = \prod_{i=0}^{n_t-1} (C_i)^{r^i}$, $I_D = \prod_{i=0}^{n_t-1} (D_i)^{r^i}$	
19: MT_IPP.Prove($crs_{MT}, C_{1-AB}, C_{2-AB}, C_C, C_D, I_{AB}, I_C, I_D$, $(A_i, B_i, C_i, D_i)_{i \in [n_t]}, \vec{r}) \rightarrow \pi_{MT}$	
20: $\pi_{agg} = (C_{1-AB}, C_{2-AB}, C_C, C_D, I_{AB}, I_C, I_D, \pi_{MT})$	
21: SnarkPack.Verify($vk^m, crs_{agg}, \{st^{m,i}\}_{i \in [n_t]}, \pi_{agg}$) $\rightarrow b_1 \wedge b_2$	
22: MT_IPP.Verify($crs_{MT}, C_{1-AB}, C_{2-AB}, C_C, C_D, I_{AB}, I_C, I_D, \vec{r}, \pi_{MT}$) $\rightarrow b_1$	
23: $(I_{AB} \stackrel{?}{=} e(g^{\alpha \sum_{i=0}^{n_t-1} r^i}, h^\beta) e(I_C^{\sum_{i=0}^{n_t-1, t} a_{i,j}}, h^\gamma) e(I_D, h^\delta)) \rightarrow b_2$	
24: $(I_{AB} \stackrel{?}{=} e(g^{\alpha \sum_{i=0}^{n_t-1} r^i}, h^\beta) e(I_D^{\sum_{i=0}^{n_t-1, t} a_{i,j}}, h^\gamma) e(I_C, h^\delta)) \rightarrow b_2$	

Fig. 11. Generating zk-SNARK proofs for relation R_{agg} .

ments Com are secure, and moreover a model is partitioned into *PriorNet* and *LaterNet* with an optimal splitting strategy, then our publicly verifiable model evaluation satisfies the following three properties:

Correctness. If *PriorNet* F_{M_1} runs on correctly encrypted inputs X_{et} and outputs $Y_{et}^{(3)}$, and meanwhile, *LaterNet* F_{M_2} runs on the correctly decrypted $Y^{(3)}$ and returns l_{test} , then l_{test} is verified and $l_{test} = F_{M_2}(F_{M_1}(X))$;

Security. If a PPT \mathcal{A} knows all public parameters and public outputs of \prod_s , L-FHE and Com , as well as, the computation of F_{M_1} and F_{M_2} , but has no access to the model parameters of F_{M_1} , it cannot generate l_{test}^* which passes verification but $l_{test}^* \neq F_{M_2}(F_{M_1}(X))$;

Privacy. If a PPT \mathcal{A} knows all public parameters and public outputs of \prod_s , L-FHE and Com , as well as, the computation of F_{M_1} and F_{M_2} , but has no access to the model parameters of F_{M_1} , it cannot obtain any information about X .

We recall that a secure CaP zk-SNARK scheme should satisfy the properties of completeness, knowledge-soundness and zero-knowledge; a secure commitment should be correct, hiding and binding, and a secure L-FHE scheme satisfies semantic security and correctness. Now we are ready to analyze how the three properties of correctness, security and privacy can be supported by the underlying used cryptographic components of our publicly verifiable model evaluation method.

Firstly, property **Correctness** relies on the correctness of L-FHE and commitments, and the completeness of the underlying CaP zk-SNARKs schemes. We employ a widely adopted L-FHE scheme [36] which has been proved correct. As for CaP zk-SNARKs schemes, our designs use (S1) Fiore et al.'s CaP zk-SNARK for simultaneous evaluation of multiple ciphertexts generated by the L-FHE scheme [21], (S2) the CaP Groth16 scheme [20], (S3) our QMP-based zk-SNARK derived from the CaP Groth16, and (S4) the CaP zk-SNARK CP_{link} for

compositing separate proofs [20]. The proposed schemes (S1), (S2) and (S4) satisfy completeness as proved.

Based on *Theorem 10* of scheme (S1) [21], we deduce the correctness of zk-SNARK proofs for relation R_{PN}^{S1} by direct verification (see Fig. 8). Specifically, if C_{L_1}, C_X are correct commitments, and for $L_1(x, y) = W(x, y) + X(x, y) + Y(x, y) = \sum_{i=0}^{d_c} \sum_{j=0}^{l_{\text{new}}^2-1} l_{i,j} x^i y^j$ and random point $k \in Z_p$, $s, t \in Z_p$, the following formula holds,

$$\begin{aligned} T(s, t) &= \frac{L_1(s, t) - L_1(k, t)}{(s - k)} \\ &= \frac{[(L_{1,0}(s) \cdot t^0 + \dots + L_{1,l_{\text{new}}^2-1}(s) \cdot t^{l_{\text{new}}^2-1}) - (L_{1,0}(k) \cdot t^0 + \dots + L_{1,l_{\text{new}}^2-1}(k) \cdot t^{l_{\text{new}}^2-1})]}{(s - k)} \\ &= \frac{[(l_{0,0}(s - k) + \dots + l_{d_c,0}(s^{d_c} - k^{d_c})) \cdot t^0 + \dots + (l_{0,l_{\text{new}}^2-1}(s - k) + \dots + l_{d_c,l_{\text{new}}^2-1}(s^{d_c} - k^{d_c})) \cdot t^{l_{\text{new}}^2-1}]}{(s - k)} \\ &= \sum_{j=0}^{l_{\text{new}}^2-1} \sum_{t=0}^{d_c-1} \sum_{i=0}^{d_c-t} l_{i+t,j} k^{i-1} s^i t^j. \end{aligned}$$

Note that C_T correctly commits to $T(s, t)$, then given $\pi^{S1} = (C_T, e, \sigma, \tau)$, a verifier can compute U which is equal to $e(h^a \bar{g}^b, g^*)$ (see line 28 in Fig. 8) by

$$\begin{aligned} U &= e(h^\sigma \bar{g}^\tau, g^*) \cdot e(C_T, g_1^*/g^{*k})^e \cdot e(C_L^1/C_{L,k}^1, g^*)^{-e} \\ &= e(h^\sigma \bar{g}^\tau, g^*) \cdot e(h^{r_T} \bar{g}^{T(s,t)}, g^{*(s-k)})^e \cdot e\left(\frac{h^{r_T}}{h^{r_{T,k}}} \frac{g^{L_1(s,t)}}{g^{L_1(k,t)}}, g^*\right)^{-e} \\ &= e(h^\sigma \bar{g}^\tau, g^*) \cdot e(h, g^*)^{e r_T(s-k)} \cdot e(g, g^*)^{e T(s,t)(s-k)} \\ &\quad e(h, g^*)^{-e(r_T - r_{T,k})} \cdot e(g, g^*)^{-e(L_1(s,t) - L_1(k,t))} \\ &= e(h, g^*)^\sigma \cdot e(h, g^*)^{e(r_T, k - r_{T,k})} \cdot e(\bar{g}, g^*)^{\tau + e r_T} \\ &\quad e(g, g^*)^{e T(s,t)(s-k)} \cdot e(g, g^*)^{-e(L_1(s,t) - L_1(k,t))} \\ &= e(h, g^*)^\sigma \cdot e(\bar{g}, g^*)^b \cdot 1 \\ &= e(h^a \bar{g}^b, g^*). \end{aligned}$$

Based on *Theorem H.1.* of (S3) [20], we proceed to derive the correctness of zk-SNARK proofs for relation $R_{\text{PN}}^{S2}[L_1]$ (see Fig. 9) by verifying $\pi^{S2} := (A, B, C, D, C'_{L_1,k})$, where $C'_{L_1,k}$ is used for CP_{Link} . Specifically, a verifier needs to verify that $(*) \text{Tr}\{e(A, B)\} \stackrel{?}{=} \text{Tr}\{e(g^\alpha, h^\beta) \cdot e(D, h^\gamma) \cdot e(C, h^\delta)\}$, where

$$\begin{aligned} \text{Tr}\{e(A, B)\} &= \text{Tr}\{e(g^\alpha \cdot g^{Z^T L(z)} \cdot g^{\delta t}, h^\beta \cdot h^{R(z)} \cdot h^{\delta s})\} \\ &= e(g, h)^{\text{Tr}\{(\alpha + Z^T L(z) + \delta t)(\beta + R(z) + \delta s)\}} \\ &= e(g, h)^{(\alpha + \delta t)(\beta + R(z) + \delta s) + \text{Tr}\{Z^T L(z)(\beta + R(z) + \delta s)\}} \\ &= e(g, h)^{(\alpha + \delta t)(\beta + R(z) + \delta s) + \beta Z^T L(z) + \text{Tr}\{Z^T L(z)R(z)\} + \delta s Z^T L(z)}, \\ \text{Tr}\{e(g^\alpha, h^\beta) \cdot e(D, h^\gamma) \cdot e(C, h^\delta)\} &= \text{Tr}\{e(g, h)^{\alpha\beta} \cdot e(g^{\frac{\beta Z^T L(z) + \alpha R(z) + Z^T O(z) + v\eta}{\gamma}}, h^\gamma) \\ &\quad \cdot e(g^{h(z, Z)t(z)/\delta + (\alpha + Z^T L(z) + \delta t)s + (\beta + R(z) + \delta s)t - ts\delta - v\eta/\delta}, h^\delta)\} \\ &= e(g, h)^{\alpha\beta + \beta Z^T L(z) + \alpha R(z) + \text{Tr}\{Z^T O(z)\} + v\eta} \\ &\quad \cdot e(g, h)^{h(z, Z)t(z) + (\alpha + Z^T L(z) + \delta t)s\gamma + (\beta + R(z) + \delta s)t\gamma - ts\gamma^2 - v\eta}. \end{aligned}$$

Due to $p(x, Z) = \text{Tr}\{Z^T \cdot L(x) \cdot R(x)\} - \text{Tr}\{Z^T \cdot O(x)\} = h(x, Z)t(x)$, formula $(*)$ holds. The presentation of the correctness of (S2) is omitted, as it can be directly found in [20]. In addition, the correctness of (S4) refers to Section 4 in [20].

Secondly, property **Security** relies on the correctness of L-FHE, and the knowledge-soundness of zk-SNARKs we leveraged. The correctness of L-FHE ensures that $\mathbf{Y}_{et}^{r(3)} = f_{\text{avg}}(f_{\text{act}}(f_{\text{conv}}(\mathbf{X}_{et}^{r(1)})))$ decrypts to $\mathbf{Y}^{r(3)} = f_{\text{avg}}(f_{\text{act}}(f_{\text{conv}}(\mathbf{X}^{r(1)})))$. In the following, based on the knowledge-soundness of [21], we majorly analyse that (1) if any adversary \mathcal{A} can provide valid proofs with regard to layer-by-layer computations, e.g., π^{S1} and π^{S2} for the first layer L_1 , there exists an extractor outputting the witnesses, e.g., $\mathbf{W}_{ed}^{r(1)}$ plus $\mathbf{X}_{et}^{r(1)}$, and $\mathbf{W}_{ed,k}^{r(1)}$ plus $\mathbf{X}_{et,k}^{r(1)}$, with all but negligible probability, for satisfying our defined relations; (2) the probability that \mathcal{A} generates $l_{\text{test}}^* = F_{M_2}(F_{M_1}(\mathbf{X}_{et}^{r(1)}))$ is negligible, that is, $d_c l_q = 4096/2^{109}$. In our case, it can be partitioned into the probability of generating $\mathbf{Y}_{et}^{r(3)*} = f_{\text{avg}}(f_s(f_{\text{conv}}(\mathbf{X}_{et}^{r(1)})))$ is negligible, and meanwhile, the probability of generating $l_{\text{test}}^* = f_o(f_{fc}(f_{fc}(f_{\text{avg}}(f_s(f_{\text{conv}}(\mathbf{Y}_{et}^{r(3)*}))))))$ is negligible.

Thirdly, the **Privacy** property relies on the the semantically security of L-FHE and the zero-knowledge of zk-SNARKs. In terms of semantically security, we derive from the security of a previously proposed L-FHE, such that for any PPT adversary \mathcal{A} , the probability of the following experiment $\text{Exp}_{\mathcal{A}}^{\text{Privacy}}[\text{L-FHE}, f_{\text{avg}}(f_s(f_{\text{conv}}(\cdot)), \lambda)]$ outputting 1 is not larger than $1/2 + \text{negl}(\lambda)$:

$$\begin{aligned} \text{Exp}_{\mathcal{A}}^{\text{Privacy}}[\text{L-FHE}, f_{\text{avg}}(f_s(f_{\text{conv}}(\cdot)), \lambda)] : \\ b \leftarrow 0, 1; \\ (pk_u, sk_u) \leftarrow \text{L-FHE.KeyGen}(1^\lambda); \\ (\mathbf{X}_0^{r(1)}, \mathbf{X}_1^{r(1)}) \leftarrow \mathcal{A}(pk_u); \\ (\mathbf{X}_{et,b}^{r(1)}) \leftarrow \text{L-FHE.Enc}(\mathbf{X}_b^{r(1)}); \\ b^* \leftarrow \mathcal{A}(pk_u, \mathbf{X}_{et,b}^{r(1)}); \\ \text{If } b^* = b, \text{ output } 1, \text{ else } 0. \end{aligned}$$

In addition, we analyse zero-knowledge based on the zero-knowledge simulators of the underlying zk-SNARKs, such as $\text{Sim}^{\text{MUniEv}-\Pi}$ and $\text{Sim}^{\text{AC}-\Pi}$, see Fig. 8 and Fig. 9, respectively. With the simulators ($\text{Sim}^{\text{MUniEv}-\Pi}, \text{Sim}^{\text{AC}-\Pi}$), we have that any PPT distinguisher \mathcal{D} successfully distinguishes the honestly generated proofs by the simulators with a negligible probability, shown as following:

$$\begin{aligned} \text{Pr}\{\text{MUniEv} - \Pi.\text{Setup}(1^\lambda, d_c, n_c) \rightarrow (ck^{S1}, \text{td}), \\ \text{MUniEv} - \Pi.\text{Prove}(ck^{S1}, \mathbf{W}_{ed}^{r(1)}, \mathbf{X}_{et}^{r(1)}) \rightarrow \pi^{S1}, \\ \text{Sim}^{\text{MUniEv}-\Pi}(\text{td}, C_{w_1}, C_X) \rightarrow \pi^{S1*}; \\ \text{AC} - \Pi.\text{Setup}(1^\lambda, QMP) \rightarrow (\text{crs}, \text{td}) \\ \text{AC} - \Pi.\text{Prove}(\text{crs}, \text{st}, \text{wt}) \rightarrow \pi^{S2}, \\ \text{Sim}^{\text{AC}-\Pi}(\text{td}, \text{st}) \rightarrow \pi^{S2*} \\ |\mathcal{D}(\pi^{S1}, \pi^{S1*} = 1 \wedge \mathcal{D}(\pi^{S2}, \pi^{S2*} = 1))\} \leq \text{negl}(\lambda). \end{aligned}$$

VI. EXPERIMENTS

Implementation. The main components of our implementation include: zk-SNARK systems, fully HE, polynomial commitment as well as simple CNNs on MNIST dataset. We firstly use the libsnark library in C++ to implement proving/verification based on Groth16 of QAPs and QMP-based circuits during the process of CNN prediction. We then use the Microsoft SEAL library to encrypt test inputs

and evaluate PriorNet on encrypted inputs, with necessary parameters setting (*i.e.*, $d_c = 4096, q = 2^{109}, t = 1032193$) as recommended. We proceed to implement the component of polynomial commitment using the libff library of libsnark, for generating commitments to encrypted/unencrypted data. Lastly, in the aspect of machine learning models, we start from a toy CNN with a convolution layer, a ReLU layer plus an average pooling layer, and generate proofs w.r.t the toy CNN running on MNIST dataset. We finally extend it to LeNet-5 over MNIST dataset. Due to the parameters and pixel values of data are floating-point numbers, not adapting to zk-SNARK systems, we use a generic 8-bit unsigned quantization technique to transform them into integers in $[0, 255]$. In addition, we conduct our experiments on a Ubuntu 18.04.6 server with a 6-core Ryzen5 processor, 7.8 GB RAM and 97.2 GB Disk space.

Evaluation. We compare QMPs-based zk-SNARK and QAP-based zk-SNARK for matrix multiplication in terms of the proving time, Setup time and CRS size, as shown Fig.12 and TABLE II. Evaluation results with regard to verification time and proof size are discussed in Appendix E. Concretely, we simulate the operations of matrix multiplication in increasing dimensions up to 200×200 padding with random integers in $[0, 10]$. Then, we generate proofs for the matrix multiplication operations using the QAPs-based and QMPs-based zk-SNARKs. Fig.12 shows that the QMPs-based zk-SNARK is efficient than the QAPs-based one in generating CRS and proof, as the matrix dimension increases. For the 200×200 matrix multiplication, the QMPs-based zk-SNARK is $17.6\times$ and $13.9\times$ faster than the QAPs-based one in Setup time and proving time, respectively. Besides, the QMPs-based zk-SNARK obviously produces smaller CRS size than the QAPs-based zk-SNARK, see TABLE II.

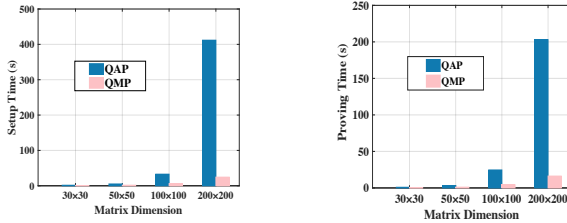


Fig. 12. Comparison on Setup time and proving time.

TABLE II
CRS SIZE COMPARISON (KB).

Matrix dimension	30 × 30	50 × 50	100 × 100	200 × 200
QAP	2,911.22	12,445.73	97,230.09	768,503.09
QMP	84.42	233.83	934.21	3,735.72

Matrix dimension	500×	1000×	2000×	3000×
QMP	23,346.32	93,384.16	373,535.53	840,454.47

We can see in Fig. 13 that the QMP-based zk-SNARK can handle the matrix multiplication in increasing dimensions up to 3360×3360 , which is its merit, compared to the QAP-based zk-SNARK supporting the maximum number of multiplication bound 10^7 [13]. Also, the proving time almost increases linearly by the dimension of matrices. We proceed

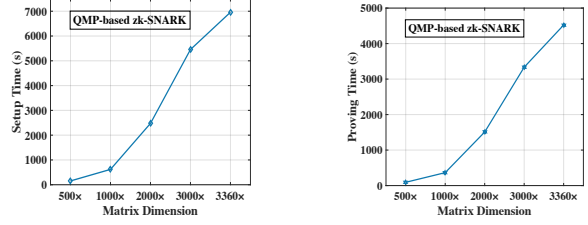


Fig. 13. Performance of our QMP-based zk-SNARK handling matrix multiplication in dimensions greater than 220×220 .

TABLE III
PERFORMANCE FOR A CONV. LAYER WITH 1000 INPUTS.

#Filter	Time (s)			Size (KB)	
	Setup	Prove	Ver	CRS	Proof
1	236.55	184.41	54559	1,054,266.00	351,421.97
3	375.88	198.75	54002	1,054,266.00	351,421.97
5	524.02	209.94	56011	1,054,266.00	351,421.97

to apply the QMP-based zk-SNARK in a convolution layer with stride (1,1), taking as inputs 1000 images of 28×28 and 1,3,5 filters of 5×5 , respectively. We transform the convolution operations into a matrix multiplication between a weight matrix and an input matrix both in dimension 3360×3360 . We note $3360 = 28 \times (28 - 5 + 1) \times 5 \approx mn^2$, where m, n mean the dimension of a filter and an image, respectively. Here, $m \geq M$ which is the number of filters. Different from the aforementioned experiments where the values of matrices are random integers, the weight matrix of 3360×3360 here is strategically assigned with the weights of filters plus some zero elements as padding, for ensuring computation correctness (recall it in Fig.5), and similarly, the input matrix of 3360×3360 is assigned with the pixel values of 1000 images, padding with $3360 \times (3360 - 1000)$ zeros. As a result, the average performance results of 5 runs are shown in TABLE III. We can see for 5 filters the Setup and proving time are 524.02s and 209.94s, respectively, which are greatly smaller than the aforementioned experiments as presented in Fig.13. The main reason can be the padding zero elements inside the weight and input matrices cancel a lot of multiplications.

We further highlight the above phenomenon by conducting additional experiments (named Exp (★)) on 1, 2, 3, 4, 5 filters and 1000, 2000, 3000, 3360 inputs, as elaborated in TABLE IV and Fig. 14. Note that the resulting CRS size and proof size

TABLE IV
PERFORMANCE OF EXPERIMENT EXP (★) (s).

	#Input	Setup Time	Proving Time	Ver. Time
One filter	1000	229.46	199.88	54313
	2000	444.25	332.61	53721
	3000	664.60	482.74	53770
	3360	753.73	541.70	54650
Five filters	1000	522.47	200.85	54933
	2000	1021.25	351.50	54646
	3000	1521.46	502.90	54367
	3360	1717.37	557.96	55204

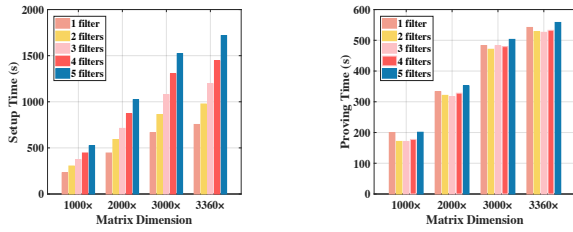


Fig. 14. Performance of experiment Exp (*)

TABLE V
PERFORMANCE FOR EXP (**) (s).

Layer	Setup Time	Proving Time	Ver. Time
ReLU	5520.61	1448.83	14.78
Pooling	196.43	49.93	14.78

in the above experiments are the same. We can see in Fig. 14 that the proving time basically stays stable regardless of the number of filters, but the Setup time increases linearly by the number of filters. We note that the complexity of the proving time is $O(mn^2)$, $m \geq M$ (resp. $O(Mn^2)$ if $m < M$), where mn^2 (resp. Mn^2) is also the number of inputs, and herein the proving time is independent of M .

We proceed to generate QAPs-based proofs for the ReLU and average pooling operations on the previous 3360×3360 matrix, named Exp (**). Note that a ReLU operation needs 20 constraints and an average pooling operation needs 144 constraints. The evaluated performance is elaborated in TABLE V.

VII. CONCLUSION

We study verifiable CNN testing over encrypted test data by leveraging the state-of-the-art zk-SNARK systems. Following existing related works, we make efforts to optimize matrix multiplication relations. Specifically, we represent convolution operations applying to multiple filters and inputs with a single MM computation. We then use a new QMP for expressing the MM computation, so as to reduce the multiplication gate of the finally generated circuit for the MM computation, and thereby reducing proof generation overhead. We also enable batch verification for reducing verification costs. We aggregate multiple proofs with respect to a same CNN but different test datasets into a single proof. Besides, we present a proof-of-concept implementation and conduct experiments to demonstrate the validity of our approach.

REFERENCES

- [1] Y. LeCun, B. Boser *et al.*, “Backpropagation applied to handwritten zip code recognition,” *Neural computation*, vol. 1, no. 4, pp. 541–551, 1989.
- [2] R. Das, E. Piciucco *et al.*, “Convolutional neural network for finger-vein-based biometric identification,” *IEEE Transactions on Information Forensics and Security*, vol. 14, no. 2, pp. 360–373, 2018.
- [3] G. Accident, “A google self-driving car caused a crash for the first time,” <https://www.theverge.com/2016/2/29/11134344/google-self-driving-car-crash-report>, 2016.
- [4] “The two-year fight to stop amazon from selling face recognition to the police,” <https://www.technologyreview.com/2020/06/12/1003482/amazon-stopped-selling-police-face-recognition-fight/>, 2020.
- [5] M. Wicker, X. Huang *et al.*, “Feature-guided black-box safety testing of deep neural networks,” in *Proc. of TACAS*, 2018, pp. 408–426.
- [6] A. Aggarwal, S. Shaikh, S. Hans, S. Halder, R. Ananthanarayanan, and D. Saha, “Testing framework for black-box ai models,” in *Proc. of IEEE/ACM ICSE-Companion*, 2021, pp. 81–84.
- [7] L. Ma, F. Juefei-Xu, F. Zhang, J. Sun, M. Xue, Li *et al.*, “Deepgauge: Multi-granularity testing criteria for deep learning systems,” in *Proc. of ACM/IEEE ICASE*, 2018, pp. 120–131.
- [8] D. Hendrycks and T. Dietterich, “Benchmarking neural network robustness to common corruptions and perturbations,” in *ICLR*, 2018.
- [9] Z. Ghodsi, T. Gu, and S. Garg, “Safetynets: Verifiable execution of deep neural networks on an untrusted cloud,” <https://arxiv.org/pdf/1706.10268.pdf>, 2017.
- [10] M. I. M. Collantes, Z. Ghodsi, and S. Garg, “Safetpu: A verifiably secure hardware accelerator for deep neural networks,” in *Proc. Of IEEE VTS*, 2020, pp. 1–6.
- [11] S. Lee, H. Ko, J. Kim, and H. Oh, “vcnn: Verifiable convolutional neural network,” <https://eprint.iacr.org/2020/584.pdf>, 2020.
- [12] B. Feng, L. Qin, Z. Zhang, Y. Ding, and S. Chu, “Zen: An optimizing compiler for verifiable, zero-knowledge neural network inferences,” <https://eprint.iacr.org/2021/087.pdf>, 2021.
- [13] J. Keuffer, R. Molva, and H. Chabanne, “Efficient proof composition for verifiable computation,” in *Proc. of ESORICS*, 2018, pp. 152–171.
- [14] L. Zhao, Q. Wang, C. Wang, Q. Li, C. Shen, and B. Feng, “Veriml: Enabling integrity assurances and fair payments for machine learning as a service,” *IEEE Transactions on Parallel and Distributed Systems*, vol. 32, no. 10, pp. 2524–2540, 2021.
- [15] A. Madi, R. Sirdey *et al.*, “Computing neural networks with homomorphic encryption and verifiable computing,” in *ACNS*, 2020, pp. 295–317.
- [16] T. Liu, X. Xie, and Y. Zhang, “zkcn: Zero knowledge proofs for convolutional neural network predictions and accuracy,” in *Proc. of ACM CCS*, 2021.
- [17] J. Thaler, “Time-optimal interactive proofs for circuit evaluation,” in *Annual Cryptology Conference*, 2013, pp. 71–89.
- [18] J. Groth, “On the size of pairing-based non-interactive arguments,” in *EUROCRYPT*, 2016, pp. 305–326.
- [19] S. Agrawal, C. Ganesh *et al.*, “Non-interactive zero-knowledge proofs for composite statements,” in *CRYPTO*, 2018, pp. 643–673.
- [20] M. Campanelli, D. Fiore, and A. Querol, “Legosnark: Modular design and composition of succinct zero-knowledge proofs,” in *Proc. of ACM CCS*, 2019, pp. 2075–2092.
- [21] D. Fiore, A. Nitulescu, and D. Pointcheval, “Boosting verifiable computation on encrypted data,” in *PKC*, no. 12111, 2020, pp. 124–154.
- [22] D. Mouris and N. G. Tsoutsos, “Zilch: A framework for deploying transparent zero-knowledge proofs,” *IEEE Transactions on Information Forensics and Security*, 2021.
- [23] “Bvlc/caffe,” <https://github.com/BVLC/caffe/wiki/Model-Zoo>, 2019.
- [24] Kaggle, “Data science competition platform,” <https://www.kaggle.com/>.
- [25] G. Xu, H. Li *et al.*, “Verifynet: Secure and verifiable federated learning,” *IEEE Transactions on Information Forensics and Security*, vol. 15, pp. 911–926, 2019.
- [26] J. Zhang, T. Liu, W. Wang, Y. Zhang, D. Song, X. Xie, and Y. Zhang, “Doubly efficient interactive proofs for general arithmetic circuits with linear prover time,” <https://eprint.iacr.org/2020/1247.pdf>, 2020.
- [27] S. Goldwasser, Y. T. Kalai, and G. N. Rothblum, “Delegating computation: interactive proofs for muggles,” *Journal of the ACM*, vol. 62, no. 4, pp. 1–64, 2015.
- [28] C. Niu, F. Wu, S. Tang, S. Ma, and G. Chen, “Toward verifiable and privacy preserving machine learning prediction,” *IEEE Transactions on Dependable and Secure Computing*, 2020.
- [29] J. Zhang, Z. Fang, Y. Zhang, and D. Song, “Zero knowledge proofs for decision tree predictions and accuracy,” in *Proc. of ACM CCS*, 2020, pp. 2039–2053.
- [30] C. Weng, K. Yang, X. Xie, J. Katz, and X. Wang, “Mystique: Efficient conversions for zero-knowledge proofs with applications to machine learning,” in *Proc. of USENIX Security*, 2021, pp. 501–518.
- [31] Y. Aono, T. Hayashi *et al.*, “Privacy-preserving deep learning via additively homomorphic encryption,” *IEEE Transactions on Information Forensics and Security*, vol. 13, no. 5, pp. 1333–1345, 2017.
- [32] Z. He, T. Zhang, and R. B. Lee, “Model inversion attacks against collaborative inference,” in *Proc. of ACSAC*, 2019, pp. 148–162.
- [33] S. G. Francesco Alesiani, “Method for verifying information,” <https://patentimages.storage.googleapis.com/53/3c/62/0ed0b3f9bb163f/US20210091953A1.pdf>, 2021.
- [34] N. Gailly, M. Maller, and A. Nitulescu, “Snarkpack: Practical snark aggregation,” <https://eprint.iacr.org/2021/529.pdf>, 2021.
- [35] R. Gennaro, C. Gentry *et al.*, “Quadratic span programs and succinct nizks without pcps,” <https://eprint.iacr.org/2012/215.pdf>, 2012.
- [36] J. Fan and F. Vercauteren, “Somewhat practical fully homomorphic encryption,” <https://eprint.iacr.org/2012/144.pdf>, 2012.
- [37] X. Chen, C. Liu *et al.*, “Targeted backdoor attacks on deep learning systems using data poisoning,” <https://arxiv.org/abs/1712.05526>, 2017.

- [38] G. Xu, H. Li *et al.*, “Secure and verifiable inference in deep neural networks,” in *Proc. of ACM ACSAC*, 2020, pp. 784–797.
- [39] Z. He, T. Zhang *et al.*, “Verideep: Verifying integrity of deep neural networks through sensitive-sample fingerprinting,” <https://arxiv.org/pdf/1808.03277>, 2018.
- [40] R. Gilad-Bachrach, N. Dowlin *et al.*, “Cryptonets: Applying neural networks to encrypted data with high throughput and accuracy,” in *ICML*, 2016, pp. 201–210.
- [41] A. E. Kosba, D. Papadopoulos *et al.*, “Trueset: Faster verifiable set computations,” in *Proc. of USENIX Security*, 2014, pp. 765–780.

APPENDIX

A. Commit-and-prove zk-SNARKs

We here particularly emphasize the capability of (CaP) zk-SNARKs. Essentially, the CaP capability allows a prover to convince a verifier of “ C_{y^1} commits to y^1 such that $y^1 = F_1(x)$ and meanwhile $y^2 = F_2(y^1)$ ”. Such capability matches our expectation, considering our scenario features as following: (a) **Compression**. Before proving the correctness of a CNN testing, the CNN developer (and testers) store commitments to the CNN (resp. test inputs), in which commitment is a lightweight method to compress large-size CNNs and test inputs, and seal them as well. (b) **Flexibility**. Committing to the CNN in advance provides the developer with certain flexibility that enables proving later-defined statements on the previously committed CNN, with regard to the test inputs which are usually later-coming. (c) **Interoperability**. The proofs corresponding to the process of CNN testing are generated separately due to that a CNN is partitioned into separate parts, so commitments to the CNN will provide the interoperability between the separately generated proofs.

B. Arithmetic constraint systems

We present here the arithmetic constraint systems of an arithmetic circuit, for complementary introduction.

Consider an arithmetic circuit containing an addition gate and two multiplication gates over the finite field F_p , that is, $a_4 := (a_1 \times a_2 + a_3) \times a_4$. It can be described by the arithmetic constraint systems as the form by $\sum a_i l_{i,op} \cdot \sum a_i r_{i,op} = \sum a_i o_{i,op}$, ($i \in [0, 4]$, $op \in [1, 2]$) with constant $a_0 = 1$ and variables $a_1, a_2, a_3, a_4 \in F_p$. Herein, $l_{i,op}, r_{i,op}, o_{i,op}$ denote the constants from F_p for the op_{th} multiplication operation; additionally, the addition operation can be handled for free.

From literature [18], such arithmetic constraint systems can be further formulated as a QAP. Specifically, suppose there are n_* multiplication operations and m variables. Now, we select t_1, \dots, t_{n_*} in F_p , and define a target polynomial $t(x) = (x - t_1) \cdots (x - t_{n_*})$. After that, we use points $\{(t_{op}, l_{i,op}), (t_{op}, r_{i,op}), (t_{op}, o_{i,op})\}_{i \in [0, m], op \in [1, n_*]}$ to accordingly construct three $(n_* - 1)$ -degree polynomials $l(x), r(x), o(x)$ via Lagrange interpolation formula. Now, we can say the mentioned arithmetic constraint systems are satisfied by $\{a_0 = 1, a_1, a_2, a_3, a_4\}$ iff the following equation holds: $\sum_{i=0}^4 a_i l_i(t_{op}) \cdot \sum_{i=0}^4 a_i r_i(t_{op}) = \sum_{i=0}^4 a_i o_i(t_{op})$, $op \in \{1, 2\}$. Informally, the QAP is composed of the polynomials $\{l_i(x), r_i(x), o_i(x)\}_{i \in [0, m]}$ and $t(x)$, where the maximal degree is $\deg(t(x)) = n_*$. Gennaro *et al.* [35] proves that there exists a $(n_{in} + n_*)$ -size QAP with degree n_* for computing a given arithmetic circuit with n_{in} inputs and n_* fan-in 2

multiplication gates whose output wires are just the outputs of the circuit.

C. Linear subspace computation

Here Fig. 15 presents the linear subspace computation $C = ck \cdot wt$ used in Fig. 10.

$$\begin{array}{c}
 \text{Linear subspace computation } C = ck \cdot wt \\
 \hline
 \begin{array}{c}
 C \in \mathbb{G}^{((l_{new}-1)^2+1)} \\
 \left[\begin{array}{c} g^{\frac{\beta}{\gamma} w_0} \cdot g^{v\eta/\gamma} \\ g^{\frac{\beta}{\gamma} w_1} \cdot g^{v\eta/\gamma} \\ \dots \\ h^{r_{w,k}} \prod_{i=0}^{(l_{new}-1)^2} \end{array} \right] \\
 wt \in \mathbb{Z}_p^{((l_{new}-1)^2+3)} \\
 \times \left[\begin{array}{c} r_{w,k} \\ v \\ w_0 \\ w_1 \\ \dots \\ W_{(l_{new}-1)^2} \end{array} \right]
 \end{array}
 =
 \begin{array}{c}
 ck \in \mathbb{G}^{((l_{new}-1)^2+1) \times ((l_{new}-1)^2+3)} \\
 \left[\begin{array}{cccccc} 0 & g^{\frac{\eta}{\gamma}} & g^{\frac{\beta}{\gamma}} & 0 & \dots & 0 \\ 0 & g^{\frac{\eta}{\gamma}} & 0 & g^{\frac{\beta}{\gamma}} & \dots & 0 \\ \dots & \dots & \dots & \dots & \dots & \dots \\ 0 & g^{\frac{\eta}{\gamma}} & 0 & 0 & \dots & g^{\frac{\beta}{\gamma}} \\ h & 0 & g_{0,0} & \dots & \dots & g_{0,(l_{new}-1)^2} \end{array} \right]
 \end{array}
 \end{array}$$

Fig. 15. Linear subspace computation.

D. Relation definition for CP_{link}

We define the relations for composite proofs, especially for that between two subsequent layers. Specifically, we define two given commitments open to the same value. We note that they are all Pedersen-like commitments.

- $C_{L_1,k}^1, C'_{L_1,k}$ open to the same $W_{et,k}^{r(1)}, X_{et,k}^{r(1)}, Y_{et,k}^{r(1)}$. $R_{PN}^{link} := \{ (st_{PN}^{link} = (C_{L_1,k}^1, C'_{L_1,k}, ck_{PN}, ck_{L_1}), wt_{PN}^{link} = (W_{et,k}^{r(1)}, X_{et,k}^{r(1)}, Y_{et,k}^{r(1)}, r_{PN}, r'_{PN})) \mid C_{L_1,k}^1 = MPoly.Com(W_{et,k}^{r(1)}, X_{et,k}^{r(1)}, Y_{et,k}^{r(1)}, r_{PN}, ck_{PN}) \wedge C'_{L_1,k} = MPoly.Com(W_{et,k}^{r(1)}, X_{et,k}^{r(1)}, Y_{et,k}^{r(1)}, r'_{PN}, ck_{L_1}) \}$.
- L_1 and L_2 use the same $Y_{et,k}^{r(1)}$: $R_{L_1,2} := \{ (st_{L_1,2} = (C_{L_2}[Y_{et,k}^{r(1)}], C'_{L_1,k}), wt_{L_1,2} = (Y_{et,k}^{r(1)}, ck_{L_1}, ck_{L_2})) \mid MPoly.OpenVer(C_{L_2}[Y_{et,k}^{r(1)}], ck_{L_2}) == MPoly.OpenVer(C'_{L_1,k}, ck_{L_1}) \}$.
- L_2 and L_3 use the same $Y_{et,k}^{r(2)}$: $R_{L_2,3} := \{ (st_{L_2,3} = (C_{L_3}[Y_{et,k}^{r(2)}], C'_{L_2,k}), wt_{L_2,3} = (Y_{et,k}^{r(2)}, ck_{L_2}, ck_{L_3})) \mid MPoly.OpenVer(C_{L_3}[Y_{et,k}^{r(2)}], ck_{L_3}) == MPoly.OpenVer(C'_{L_2,k}, ck_{L_2}) \}$.
- L_3 and L_4 use the same $Y^{r(3)}$: $R_{L_3,4} := \{ (st_{L_3,4} = (C_{Y^{r(3)}}^{inter}, C_{PN}^{inter}), wt_{L_3,4} = (Y^{r(3)}, Y_{et,k}^{r(3)}, ck_{L_3}, ck_{L_4})) \mid Enc(MPoly.OpenVer(C_{Y^{r(3)}}^{inter}, ck_{L_4})) == MPoly.OpenVer(C_{PN}^{inter}, ck_{L_3})[Y_{et,k}^{r(3)}] \}$.
- L_4 and L_5 use the same $Y^{r(4)}$: $R_{L_4,5} := \{ (st_{L_4,5} = (C_{L_5}[Y^{r(4)}], C_{Y^{r(4)}}), wt_{L_4,5} = (Y^{r(4)}, ck_{L_4}, ck_{L_5})) \mid MPoly.OpenVer(C_{L_5}[Y^{r(4)}], ck_{L_5}) == MPoly.OpenVer(C_{Y^{r(4)}}^{inter}, ck_{L_4}) \}$.
- L_5 and L_6 use the same $Y^{r(5)}$: $R_{L_5,6} := \{ (st_{L_5,6} = (C_{L_6}[Y^{r(5)}], C'_{L_5,k}), wt_{L_5,6} = (Y^{r(5)}, ck_{L_5}, ck_{L_6})) \mid MPoly.OpenVer(C_{L_6}[Y^{r(5)}], ck_{L_6}) == MPoly.OpenVer(C_{textbf{Y}^{r(5)}}, ck_{L_5}) \}$.

- L_6 and L_7 use the same $\mathbf{Y}^{r(6)}$: $R_{L_{6,7}} := \{(\mathbf{st}_{L_{6,7}} = (C_{L_7}[\mathbf{Y}^{r(6)}], C_{\mathbf{Y}^{r(6)}}), \mathbf{wt}_{L_{6,7}} = (\mathbf{Y}^{r(6)}, ck_{L_6}, ck_{L_7})) \mid \text{MPoly.OpenVer}(C_{L_7}[\mathbf{Y}^{r(6)}], ck_{L_7}) = \text{MPoly.OpenVer}(C_{\mathbf{Y}^{r(6)}}, ck_{L_6})\}$.
- L_8 and L_o use the same $\mathbf{Y}^{r(8)}$: $R_{L_{8,o}} := \{(\mathbf{st}_{L_{8,o}} = (C_{L_o}[\mathbf{Y}^{r(8)}], C_{\mathbf{Y}^{r(8)}}), \mathbf{wt}_{L_{8,o}} = (\mathbf{Y}^{r(8)}, ck_{L_7,8}, ck_{L_o})) \mid \text{MPoly.OpenVer}(C_{L_o}[\mathbf{Y}^{r(8)}], ck_{L_o}) = \text{MPoly.OpenVer}(C_{\mathbf{Y}^{r(8)}}, ck_{L_7,8})\}$.

E. Discussion

Complementary experimental results. In terms of verification time and proof size, the QMPs-based zk-SNARK has a higher overhead than the QAPs-zk-SNARK. Its verification time grows faster than that of QAPs-based zk-SNARK, see TABLE VI. The proof size also becomes larger when the matrix dimension turns larger as shown in TABLE VIII, while the proof size in the QAPs-based zk-SNARK keeps 1019 bits regardless of the matrix dimension. We next see how the proof size becomes longer with the dimension-increasing matrices. We note that the bounded number of multiplications the QAPs zk-SNARK can handle is $220 * 220 * 220 = 10,648,000$, and then the QAPs zk-SNARK would be called multiple times when handling the multiplication operations more than 10,648,000, which results in multiple 1019-bit proofs. Suppose that the QAPs-based zk-SNARK proofs for the 3000×3000 matrix multiplication are totally $\frac{3000*3000*3000}{220*220*220} \times 1019$ bits. Also, the QMPs-based zk-SNARK proofs for the same matrix multiplication are 2,295,000,764 bits. The size is nearly 888 times of magnitude larger than the above one generated by the QAPs-based zk-SNARK. We observe that the times of magnitude become smaller as the matrix dimension increases, see TABLE VII. Thus, we suggest that the QMPs-based zk-SNARK can be more suitable to handle the matrix multiplication in a larger dimension, and in the case, the times of magnitude might approximate to zero.

TABLE VI
VERIFICATION TIME COMPARISON (S).

Matrix dimension	30×30	50×50	100×100	200×200
QAP	0.005	0.007	0.014	0.044
QMP	4.896	13.580	54.630	215.800

TABLE VII
TIMES OF MAGNITUDE IN PROOF SIZE.

Matrix dimension	$1000 \times$	$2000 \times$	$3000 \times$	$3360 \times$	$4000 \times$
Times	2665	1332	888	793	666

In our future work, we would introduce a random sampling strategy in the phase of proof generation, aiming to reduce the verification time. A straightforward idea can be adopted by randomly sampling a bounded number of values in two matrices to be multiplied, and resetting the non-chosen values as zeros. In such a way, only the sampled values in the two matrices are multiplied and only their multiplication correctness need to be proved. But here two noteworthy issues should be considered: (1) how to generate the randomness

TABLE VIII
PROOF SIZE OF THE QMPs-BASED ZK-SNARK FOR MATRIX MULTIPLICATION (KB).

Matrix dimension	30×30	50×50	100×100	200×200
Size	28.10	77.91	311.37	1,245.21
Matrix dimension	$500 \times$	$1000 \times$	$2000 \times$	$3000 \times$
Size	7,782.08	31,128.02	124,511.81	280,151.46

used for sampling against a distrusted prover; (2) how to determine the bound of the number of sampled values for ensuring computational soundness in zk-SNARKs.

Complementary explanation for Fig. 5. In Section IV-B, for ease of presentation, we assume the number of filters M is more than the dimension of a filter matrix m within a convolutional layer, and as a result, both of the transformed matrices for the filter matrices and input matrices are in dimension $Mn^2 \times Mn^2$. Herein, we add the complementary explanation for the case where the number of filters M is not more than the dimension of a filter matrix m . In this case, the transformed matrices are in dimension $mn^2 \times mn^2$, as elaborated in Fig. 16. Note that the number of inputs is mn^2 here. For the convolutional layers during a CNN testing, we would take into account the number of filters, the dimension of filter and input, as well as the number of inputs, and then strategically reshape the filters and inputs into two square matrices in the same dimension.

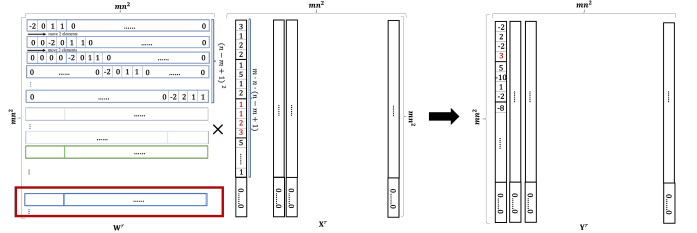


Fig. 16. Matrix multiplication for convolution operations ($M \leq m$).